

## **A New Archaeocete and Other Marine Mammals (Cetacea and Sirenia) from Lower Middle Eocene Phosphate Deposits of Togo**

Authors: Gingerich, Philip D., and Cappetta, Henri

Source: Journal of Paleontology, 88(1) : 109-129

Published By: The Paleontological Society

URL: <https://doi.org/10.1666/13-040>

---

The BioOne Digital Library (<https://bioone.org/>) provides worldwide distribution for more than 580 journals and eBooks from BioOne's community of over 150 nonprofit societies, research institutions, and university presses in the biological, ecological, and environmental sciences. The BioOne Digital Library encompasses the flagship aggregation BioOne Complete (<https://bioone.org/subscribe>), the BioOne Complete Archive (<https://bioone.org/archive>), and the BioOne eBooks program offerings ESA eBook Collection (<https://bioone.org/esa-ebooks>) and CSIRO Publishing BioSelect Collection (<https://bioone.org/csiro-ebooks>).

Your use of this PDF, the BioOne Digital Library, and all posted and associated content indicates your acceptance of BioOne's Terms of Use, available at [www.bioone.org/terms-of-use](http://www.bioone.org/terms-of-use).

Usage of BioOne Digital Library content is strictly limited to personal, educational, and non-commercial use. Commercial inquiries or rights and permissions requests should be directed to the individual publisher as copyright holder.

---

BioOne is an innovative nonprofit that sees sustainable scholarly publishing as an inherently collaborative enterprise connecting authors, nonprofit publishers, academic institutions, research libraries, and research funders in the common goal of maximizing access to critical research.



# A NEW ARCHAEOCETE AND OTHER MARINE MAMMALS (CETACEA AND SIRENIA) FROM LOWER MIDDLE EOCENE PHOSPHATE DEPOSITS OF TOGO

PHILIP D. GINGERICH<sup>1</sup> AND HENRI CAPPETTA<sup>2</sup>

<sup>1</sup>Department of Earth and Environmental Sciences, Museum of Paleontology, University of Michigan, Ann Arbor, Michigan, 48109-1079, USA, <gingeric@umich.edu>; and <sup>2</sup>Equipe Paléontologie, UMR 5554 Institut des Sciences de l'Évolution, Université de Montpellier II – Sciences et Techniques du Languedoc, Place Eugène Bataillon, 34095 Montpellier Cedex 5, France, <henri.cappetta@univ-montp2.fr>

**ABSTRACT**—Lutetian lower middle Eocene phosphate deposits of Kpogamé-Hahotoé in Togo yield new information about whales and sea cows in West Africa. Most specimens are individual teeth and bones, collected as isolated elements, but some appear to have been associated. Most are conservatively interpreted to represent a new 300–400 kg protocetid archaeocete, *Togocetus traversei*. This genus and species is distinctly primitive for a protocetid in retaining a relatively small mandibular canal in the dentary and retaining a salient metaconid on the lower first molar (M<sub>1</sub>), but it is derived relative to earlier archaeocetes in having large, dense, osteosclerotic tympanic bullae. Mandibular canal size and large dense bullae are not as tightly linked in terms of function in hearing as previously thought. Postcranially *Togocetus traversei* had many characteristics found in other semiaquatic protocetids: a relatively long neck, mobile shoulder, digitigrade manus, large pelvis, well-developed hind limbs, and feet specialized for swimming. Loss of a fovea on the head of the femur indicates loss of the teres ligament stabilizing the hip, which is a derived specialization consistent with life in water. Protocetid specimens distinctly smaller and larger than those of *Togocetus traversei* indicate the presence of at least three protocetids at Kpogamé. Sirenian vertebral and rib pieces indicate the presence of a protosirenid and a dugongid. Finally, a vertebral centrum and piece of humerus appear to represent a large land mammal. A diverse fauna of archaic whales and early sirenians inhabited the western margin of Africa and the eastern Atlantic Ocean as early as 46–44 million years before present, showing that both cetaceans and sirenians were widely distributed geographically by this time.

## INTRODUCTION

**M**OST EARLY archaeocete whales are known from Eocene deposits on the southern and eastern margins of the Tethys Sea in Egypt, India, and Pakistan (Fraas, 1904; Stromer, 1908; Sahni and Mishra, 1975; Gingerich et al., 1983, 1994, 2001a, 2001b, 2009; Kumar and Sahni, 1986; Thewissen et al., 1994, 1996; Bajpai and Gingerich, 1998; Madar et al., 2002; Nummela et al., 2006; Madar, 2007). Early sirenians are known from the northern Atlantic Ocean (Owen, 1855; Domning et al., 1982; Domning, 2001; Astibia et al., 2010; Hautier et al., 2012) and from the Tethys Sea (Owen, 1875; Abel, 1907; Zalmout et al., 2003; Zalmout and Gingerich, 2012; Bajpai et al., 2006, 2009). This makes exceptional geographic records of early archaeocetes, like those described here from Kpogamé-Hahotoé in Togo (Fig. 1), especially important. A protocetid archaeocete is known from a contemporary or later African-Atlantic site at Ameki in southeastern Nigeria (Andrews, 1920; Gingerich, 2010), basilosaurid archaeocetes are known from later African-Atlantic sites in Senegal and Morocco (Elouard, 1981; Adnet et al., 2010), and a primitive sirenian has recently been reported from a phosphate mine at Taïba Ndiaye in Senegal (Hautier et al., 2012). However, this is the first substantial marine mammal fauna to be described from the middle Eocene of the west coast of Africa and eastern margin of the Atlantic Ocean.

Kpogamé-Hahotoé, or here Kpogamé, is a phosphate mining area in Togo located some 20 km northeast of the capital city of Lomé (Fig. 2). It occupies a band about 2 km wide stretching from Aveta in the southwest to Dagbati in the northeast, a distance of some 35 km. The area is coastal, with low relief, and the surface is generally forested. Phosphate deposits were discovered by subsurface drilling in 1952, and commercial production started in 1960 or 1961. Beds are essentially flat-

lying, and the 2–6 m thick bed of commercial-grade phosphate is exploited by strip mining. Kpogamé and Hahotoé are each large, shallow, open-pit mines. Hahotoé was opened in 1959 and achieved maximum production in 1972. Kpogamé was opened in 1973. Some 14–15 million cubic meters of overburden are removed annually, and stripping is economical to a depth of about 30 meters.

Vertebrate fossils from Togo were first described by Stromer (1910), who reported 11 species of selachians from the Paleocene and Eocene. Most of the mammalian specimens from phosphate deposits at Kpogamé-Hahotoé described here were collected over the course of many years by mining-operations engineer Michel Traverse. Additional specimens were collected by one of us (HC) during field work in September–October 1985. The quality of the bone of most specimens is excellent, but all were collected as isolated elements. Similarity of preservation and rarity of duplication of most elements identified as *Togocetus traversei*, n. gen. n. sp., suggest that many of the best preserved bones may represent a single individual skeleton. Most archaeocete elements from Kpogamé-Hahotoé are interpreted, conservatively, as representing a single species. Some bones studied here have tooth marks on the surface suggesting predation or scavenging before burial. Superimposed on this, many bones were broken by heavy equipment used to extract the phosphate.

A preliminary report on selachians from Kpogamé-Hahotoé was published by Cappetta and Traverse (1988), and an abstract on the cetaceans and sirenians was published by Gingerich et al. (1992). Bourdon and Cappetta (2012) recently described remains of the pseudotoothed bird ?*Gigantornis* from Kpogamé.

Institutional abbreviations.—GSP-UM, Geological Survey of Pakistan-University of Michigan collection, presently in Ann

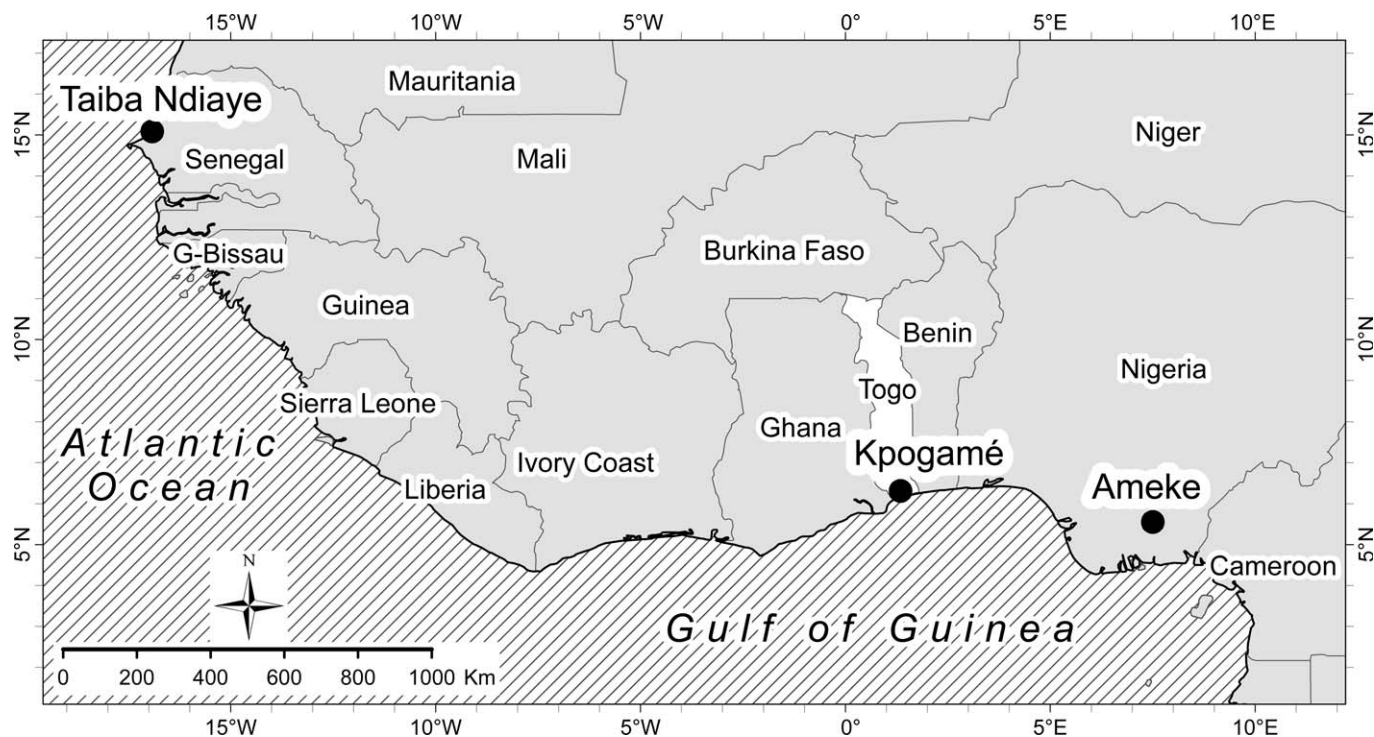


FIGURE 1—Map of West Africa showing the location of Kpogamé-Hahotoé in Togo, source of middle Lutetian *Togocetus traversei* n. gen. n. sp., and other middle Eocene protocetid and dugongid specimens described here. Taiba Ndiaye is a phosphate quarry in Senegal that has yielded a vertebra of a possible middle Eocene prorastomid sirenian (Hautier et al., 2012). Ameke in Nigeria is the source of the Lutetian or Bartonian middle Eocene protocetid *Pappocetus lugardi* Andrews (1920; Halstead and Middleton, 1974, 1976). Fossils from all three localities were deposited in tropical Atlantic waters on the western margin of the African continent.

Arbor, Michigan, U.S.A.; SMNS, Staatliches Museum für Naturkunde, Stuttgart, Germany; KPG-M and KPO-M, Université de Montpellier, Institut des Sciences de l'Évolution paleontology collection, Montpellier, France (see below).

#### STRATIGRAPHY

The Kpogamé-Hahotoé phosphate beds are in a shallow veneer of sedimentary strata overlying Precambrian basement rocks. The sedimentary strata include first a Tabligbo Group consisting of 1) Maastrichtian sands with an intermediate limestone (total ~40 m); 2) Paleocene limestones (6 m), with ostracods typical of the Ewekoro Formation in Nigeria (planktonic foraminiferal zone P3 or Selandian); and 3) lower Eocene claystones that become increasingly palygorskite-rich, ending with claystones containing ostracods and benthic and planktonic foraminifera of Ypresian age (P6 or early Ypresian). The principal references on the phosphate-bearing strata of Togo are Slansky (1962, 1980), Kilinc and Cotillon (1977), and Johnson et al. (2000).

The Kpogamé-Hahotoé phosphate complex itself (Fig. 3) overlies the Tabligbo Group. The phosphate complex has three parts, from bottom to top: 1) a lower Eocene marl-phosphate unit (~10–15 m thick in the area where phosphate is being mined) with benthic and planktonic foraminifera of P7–P8 middle-to-late Ypresian age ('*Couche-2 and 3*' in mining nomenclature; 'Clays with phosphate' here); 2) a middle Eocene phospharenite ('*Couche-1*' with bonebeds BBM and BBR; 1–8 m thick) rich in selachian teeth of Lutetian age grading laterally into a more calcareous zone of calcareous phosphate; and 3) an upper oxidized clayey phosphate unit ('*Couche-0*'; 1 m thick) lacking fossils. All are overlain by 'Continental terminal' consisting of surficial gravels, sands, and clays.

Cappetta and Traverse (1988) recovered selachian faunas from four levels in the Kpogamé-Hahotoé phosphate complex, again from bottom to top: 1) a limited fauna from the ME 644 level within the lower marl-phosphate unit, accessible only in subsurface cores; 2) a large and diverse selachian fauna from the "bone-bed du mur" (bone bed of the wall; BBM in Fig. 3) near the base of the phospharenite and continuing along the base of the calcareous zone; 3) two similar faunas, one from the "bone bed reposant sur la couche carbonatée" (bone bed resting on the carbonatized and phosphatized bed; BBR in Fig. 3) of the calcareous zone, and the other from a test trench (TR36) near the top of the calcareous zone; and 4) a fauna from the oxidized clay-phosphate unit. Faunas from the BBM and TR36 levels bracketing the calcareous zone lateral to the phospharenite show it to be middle Eocene in age, rather than Paleocene, refuting the idea that phosphate was trapped behind a previously existing coastal barrier (Kilinc and Cotillon, 1977). Johnson et al. (2000) corroborated Cappetta and Traverse's interpretation of a more open coastal environment.

Some mammalian remains, distinguished by their chalky white color, came from the lower BBM bone bed, but most of the mammalian fossils described here came from the higher BBR bone bed. There is no notable difference in comparable elements found in the two intervals. Cappetta and Traverse (1988, p. 364) mentioned planktonic foraminifera dating the phospharenite at BBM to planktonic foraminiferal zone P11 (middle Lutetian), and the vertebrate fossils described here are consistent with a middle Lutetian age as well (ca. 47–44 Ma; Berggren and Pearson, 2005; 46–43 Ma; Vandenberghe et al., 2012).

#### SYSTEMATIC PALEONTOLOGY

Specimens described here are archived in the Laboratoire de Paléontologie, Institut des Sciences de l'Évolution, at the

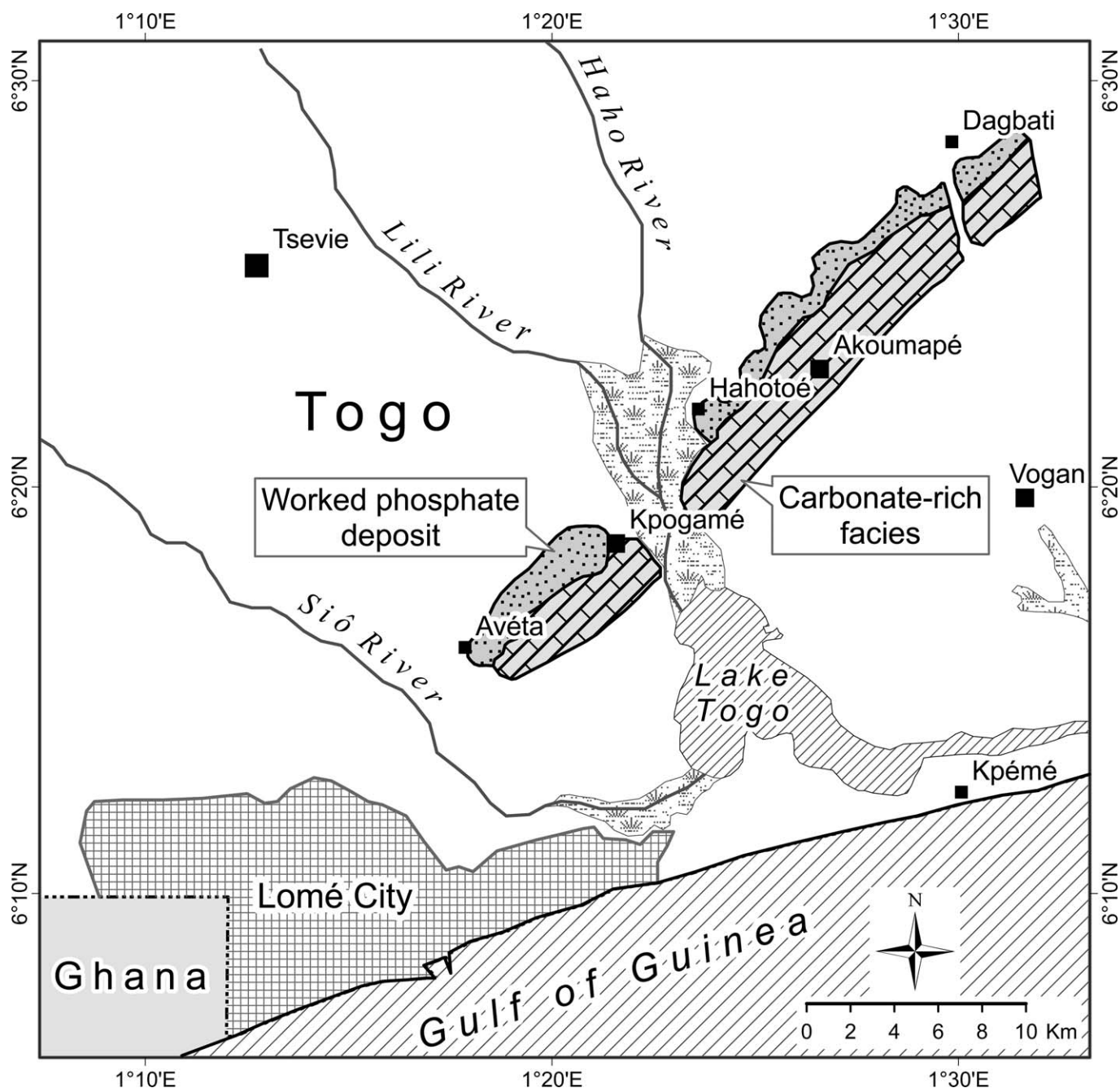


FIGURE 2—Detailed map of southern Togo showing the geographic distribution of worked phosphate deposits in relation to more carbonate-rich facies that are not exploited economically. Deposits are bisected by tributaries of Lake Togo, which are flanked by the mining settlements of Kpogamé and Hahotoé. The strike of phosphate-bearing beds is southwest-northeast, and dip is about  $1^\circ$  to the southeast. Fossils described here were collected near Kpogamé, which is located about 20 km northeast of the capital city of Lomé. A stratigraphic cross section near Kpogamé is shown in Figure 3.

Université de Montpellier II—Sciences et Techniques du Languedoc, (France). Each is numbered with the prefix KPG-M for specimens from the “bone bed reposant sur la couche carbonatée” (BBR), or KPO-M for mammalian specimens from the “bone-bed du mur” (BBM): as, for example, specimens KPG-M 1 or KPO-M 5 described here.

Order CETACEA Brisson, 1762  
 Family PROTOCETIDAE Stromer, 1908  
 Subfamily PROTOCETINAE Stromer, 1908  
 TOGOCETUS new genus

*Type species.*—*Togocetus traversei* n. sp. by monotypy.  
*Diagnosis.*—As for species.  
*Etymology.*—Named for Togo, the country of origin, and *cetus*, Gr., masc., whale.

#### TOGOCETUS TRAVERSEI new species

- 1988 *Pappocetus* (partim), CAPPETTA AND TRAVERSE, p. 362.  
 1992 “Cetacean”, GINGERICH, CAPPETTA, AND TRAVERSE, p. 29.  
 1998 “Togo whale”, WILLIAMS, p. 16.

*Diagnosis.*—Distinctive among protocetine protocetids in

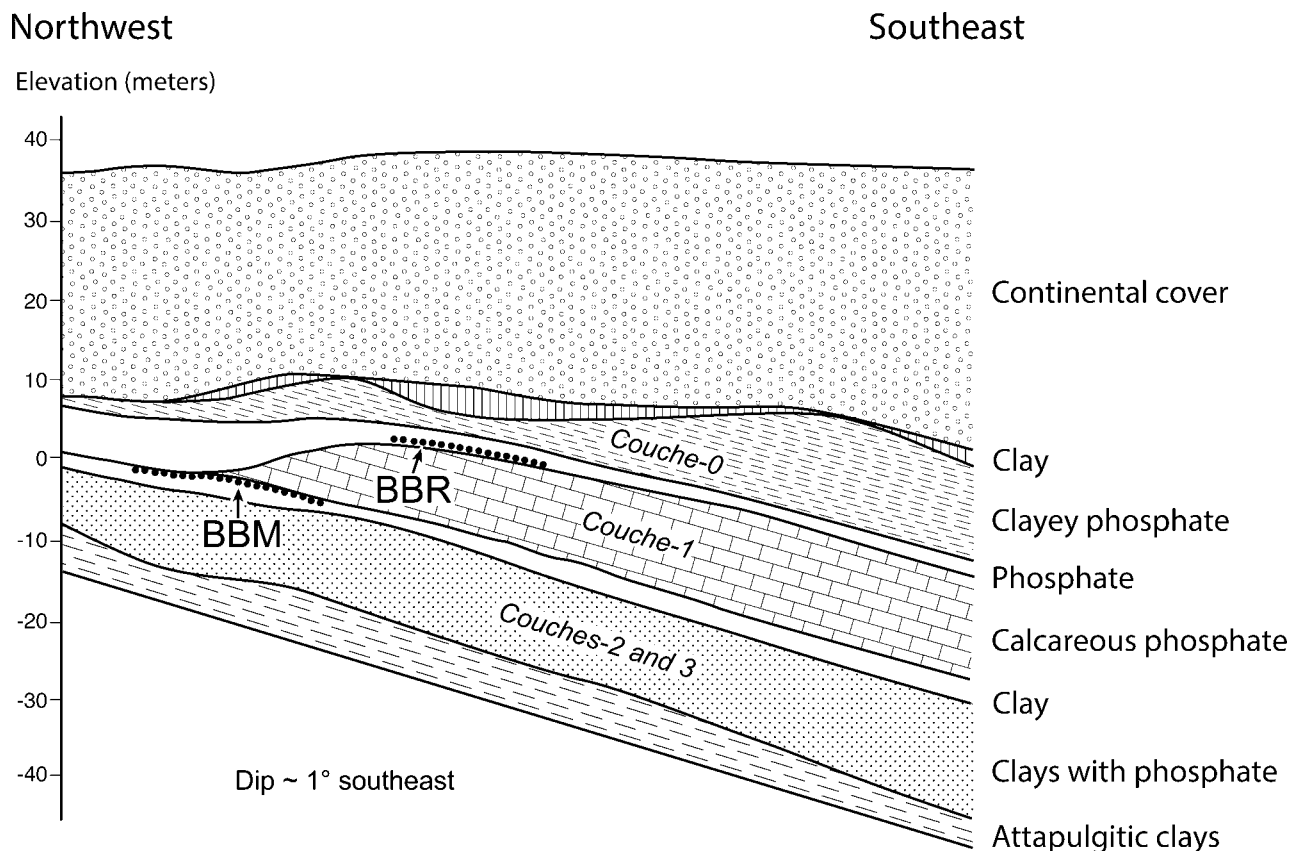


FIGURE 3—Schematic northwest-southeast cross section of phosphate-bearing strata exposed near Kpogamé (see map in Fig. 2). The phosphate complex has three parts of interest here, numbered 0, 1, and 2–3 by miners, from top to bottom: *Couche-0* is a thin oxidized clayey phosphate unit lacking fossils; *Couche-1* is a middle Eocene phospharenite rich in selachian teeth of Lutetian age with two bonebeds, BBM and BBR yielding the specimens described here; *Couches-2 and 3* are upper and lower parts of a lower Eocene marl-phosphate unit with benthic and planktonic foraminifera of P7–P8 middle-to-late Ypresian age. All are overlain by ‘Continental terminal’ consisting of surficial gravels, sands, and clays. Vertical scale is exaggerated relative to horizontal scale.

having a relatively small mandibular canal (see Fig. 6.5), retaining a salient metaconid on the trigonid of  $M_1$  (Fig. 5.13, below), and lacking a fovea for the teres ligament on the femoral head.

*Togocetus* is similar to *Protocetus* in the limited number of features that can be compared, but clearly differs from *Protocetus* in having a caniniform upper canine ( $C^1$ ), a higher-crowned  $P^4$  with no metacone, and a higher-crowned  $M^2$  with the metacone positioned closer to the apex of the crown and the crown still bearing a distinct protocone on the posterolingual base of the crown. *Togocetus* differs too in the shape of the axis vertebra ( $C_2$ ). The axis of *Togocetus* has large pits for ligaments on the dorsal surface of the dens, and a broad hypapophysis. Both axes known for *Protocetus* (SMNS 11085, 11089; Fraas, 1904; Stromer, 1908) lack the pits and have a narrowly constricted hypapophysis. *Togocetus* differs from *Pappocetus* from Nigeria (Andrews, 1920) in having a shorter and relatively broader  $M_1$ , only one-half the length of the latter. It differs from *Pappocetus* in lacking the pronounced crenulated enamel with rugose surface texture, prominent cingula, and lobate molar apices said to characterize pappocetines (McLeod and Barnes, 2008).

**Description.**—The deciduous dentition, permanent dentition, cranial elements, vertebrae, ribs, forelimb elements, and hind limb elements of *Togocetus traversei* are described separately and in detail below. We use ‘anterior’ as a term relative to the whole animal, including ‘distal’ relative to individual teeth in life position, ‘rostral’ relative to the cranium, and ‘cranial’ for postcranial elements. ‘Posterior’ is again relative to the whole animal, meaning ‘proximal’ relative to individual teeth, and

‘caudal’ relative to the cranium or postcranial elements. We use ‘medial’ and ‘lateral’ to represent elements closer to and farther from the midline of the skeleton. In the dentition ‘lingual’ is generally also medial, and ‘labial’ (for anterior teeth) and ‘buccal’ (for posterior teeth) are also lateral. ‘Ventral’ is toward the surface of the skull and body closest to earth’s surface, and ‘dorsal’ is the opposite. Descriptive terminology follows Mead and Fordyce (2009) whenever possible.

**Etymology.**—Named for the late Michel Traverse of Bourg de Lignerolles in France, who collected many of the specimens described here while working as an operations engineer at Kpogamé.

**Type.**—Holotype, KPG-M 1, left dentary with  $M_3$  (Fig. 6.4, 6.5, below). Type locality is the highly fossiliferous stratigraphic level near the top of mining level *Couche-1*, the “bone-bed reposant” (BBR), at Kpogamé-Hahotoé (6.309°N latitude, 1.334°E longitude), in Togo, West Africa.

**Occurrence.**—Planktonic foraminiferal zone P11 in the middle Lutetian, middle Eocene (Cappetta and Traverse, 1988; zone E9 of Berggren and Pearson, 2005). *Togocetus traversei* is known only from the type locality.

**Referred specimens.**—Most specimens described here; see Figures 4–12 and Tables 1–3.

**Deciduous dentition.**—Protocetid archaeocetes have a deciduous dental formula of 3.1.4 / 3.1.4, with three incisors, one canine, and four premolar teeth in each quadrant. The deciduous dentition of protocetids is simpler than the permanent dentition in having only eight teeth in each quadrant, and a total of 16 different morphologies (considering that left and right teeth are generally

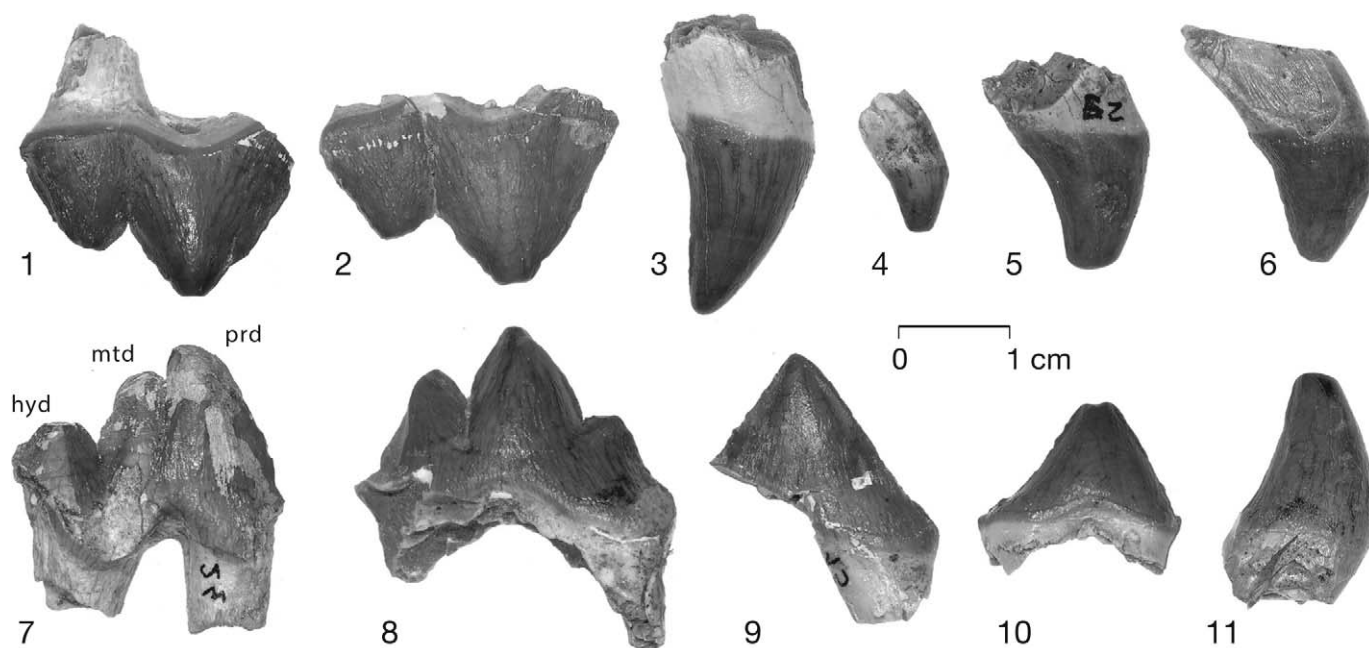


FIGURE 4—Deciduous teeth of middle Lutetian *Togocetus traversei*, n. gen. n. sp., from Kpogamé-Hahotoé. All specimens are shown as if in right lateral view and may be parts of a single individual. Upper teeth (from back to front): 1, KPG-M 10, left  $dP^4$  (reversed); 2, KPG-M 133, right  $dP^3$ ; 3, KPG-M 27, right  $dC^1$ ; 4, KPG-M 30, right  $dI^3$ ; 5, KPG-M 29, right  $dI^2$ ; 6, KPG-M 11, left  $dI^1$  (rev.); lower teeth (from back to front): 7, KPG-M 24, left  $M_1$  (rev.); 8, KPG-M 23, left  $dP_4$  (rev.); 9, KPG-M 15, left  $dP_3$ ; 10, KPG-M 16, right  $dP_2$ ; 11, KPG-M 25, right  $dC_1$ . Note the long crown of  $dP_4$  (Fig. 4.8) which is missing much of the fourth cusp or hypoconid.  $M_1$  is illustrated here because its preservation matches that of the deciduous teeth and it may be part of the same individual. Abbreviations: *hyd*=hypoconid; *mtd*=metaconid; *prd*=protoconid.

mirror images of each other). Twelve teeth representing 11 different morphologies can be identified with confidence in the known deciduous dentition of *Togocetus traversei*. Deciduous teeth of mammals generally have thinner enamel that is lighter in color, here more yellow than brown, compared to the thicker and darker enamel of permanent teeth. Deciduous teeth of *T. traversei* were identified to tooth position using the complete deciduous dentition of an undescribed protocetid for comparison (GSP-UM 3071). Most are slightly worn, which also helps in identifying their position. Representative upper and lower teeth constituting a right deciduous dentition are illustrated in Figure 4. Teeth known only from the left side have been reversed for consistency.

KPG-M 11 (Fig. 4.6) and KPG-M 29 (Fig. 4.5) are deciduous upper incisors, interpreted as  $dI^1$  and  $dI^2$ . These have simple crowns that are slightly concave lingually and slightly convex labially. Each has a single root that is elliptical in cross-section, dense, and angled sharply posteriorly when the crown is oriented vertically. Enamel is faintly crenulated. KPG-M 30 (Fig. 4.4), right  $dI^3$ , is similar to  $dI^1$  and  $dI^2$  but differs in being much smaller. KPG-M 27 (Fig. 4.3) is a right deciduous upper canine,  $dC^1$ , that is similar in form but larger and higher-crowned, with a more sharply pointed crown than that of the preceding incisors. There is no  $dP^1$  preserved in the Togo material, and it is uncertain whether protocetid archaeocetes had a  $dP^1$ . Similarly, there is no  $dP^2$  preserved in this material.

KPG-M 133 (Fig. 4.2) is the crown of a right  $dP^3$ . This was double rooted and has a large buccally positioned paracone followed by a smaller metacone. There is no protocone preserved on this tooth and it is doubtful whether *Togocetus* had a protocone on  $dP^3$  because there is no dorsal deflection of the lingual part of the faint cingulum surrounding the base of the crown. KPG-M 10 (Fig. 4.1) and KPG-M 58 are partial crowns of double-rooted left and right  $dP^4$ . The former is similar to  $dP^3$  in lateral view, but both differ from  $dP^3$  in having a small but distinct swelling and

deflection of the lingual cingulum indicating the presence of a rudimentary protocone.

KPG-M 25 (Fig. 4.11) is the crown of a right lower deciduous canine,  $dC_1$ . This was single rooted and resembles the crown of  $dC^1$  in form. It differs in being slightly smaller (and the tip of the crown is slightly worn).

KPG-M 16 (Fig. 4.10) is the crown of a right  $dP_2$  with a single prominent central cusp. The tooth was double rooted. The crown is narrow, slightly concave lingually and slightly convex labially. The sloping crest of the crown anterior to the central cusp is straight, while that posterior to the central cusp is distinctly concave. KPG-M 15 (Fig. 4.9) is the crown of  $dP_3$ , which is larger but otherwise closely similar to that of  $dP_2$ . The sloping crest of the crown posterior to the central cusp on  $dP_3$  has very faintly developed cusplules. KPG-M 23 (Fig. 4.8) is much of the crown of a left  $dP_4$ . It is unusually long, and has four substantial cusps aligned anteroposteriorly. These are clearly homologous with the paraconid, protoconid, metaconid, and hypoconid (missing here), respectively, on lower molars. The paraconid is the smallest of the three preserved cusps, the protoconid is the largest, and the metaconid is intermediate in size. The apex of the protoconid has a striated wear facet indicating that it was pulled up and back against a cusp on  $dP^3$  in front of it. The roots of  $dP_4$  are splayed and largely resorbed, suggesting that the tooth was shed when replaced by a permanent  $P_4$ .

Measurements of all deciduous teeth are included in Table 1.

**Permanent dentition.**—There are more than 50 teeth representing the permanent dentition of *Togocetus traversei*, but many of these are isolated caniniform teeth (incisors and canines) of uncertain tooth position, and others are broken or worn. Thus there are relatively few informative teeth represented. Many isolated teeth are difficult to identify to tooth position, and here this was attempted using teeth in maxillae and dentaries of *Rodhocetus kasranii* (GSP-UM 3012; Gingerich et al., 1994), *Artiocetus clavis* (GSP-UM 3458; Gingerich et al., 2001a), and



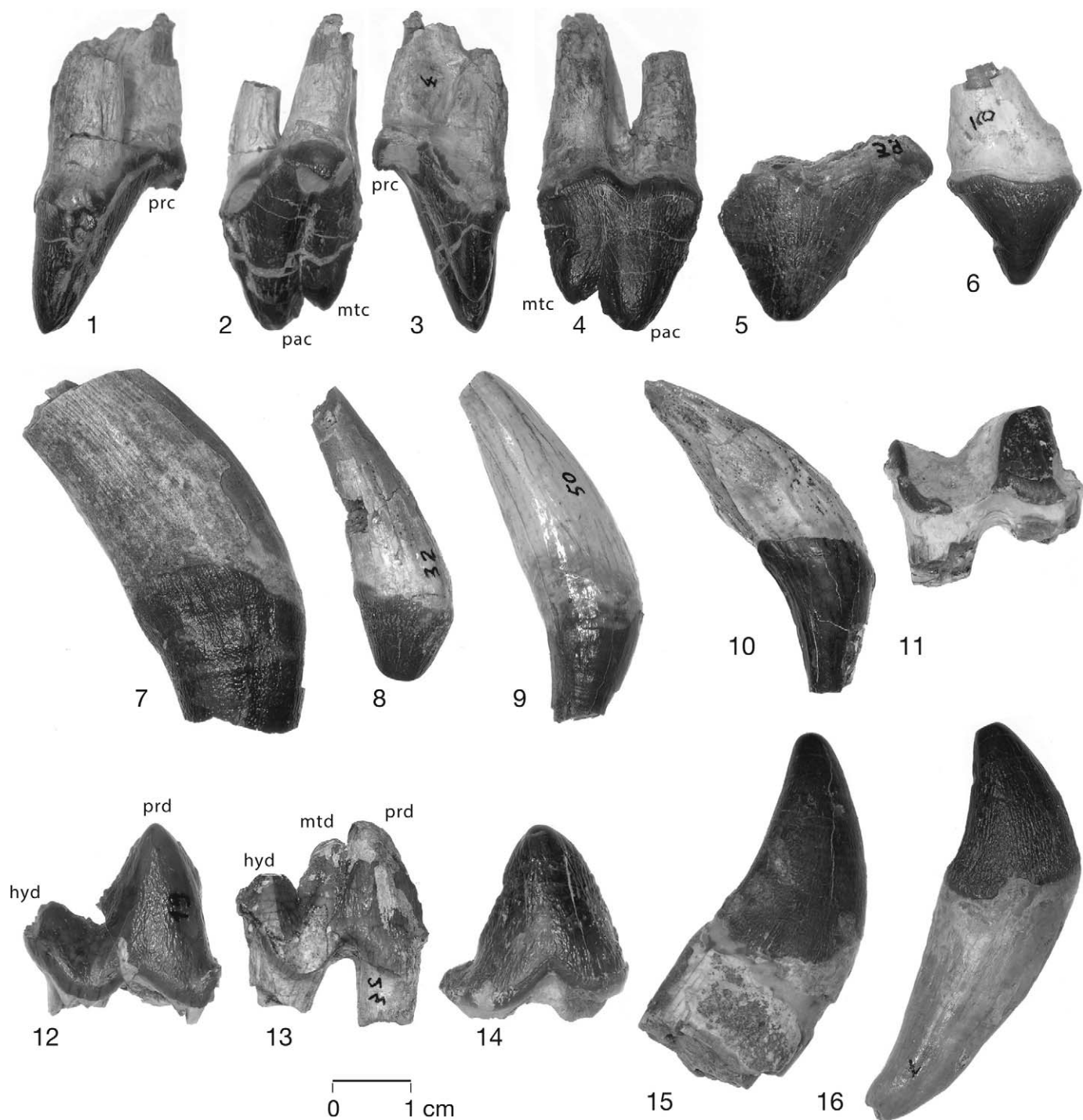


FIGURE 5—Permanent teeth of middle Lutetian *Togocetus traversei*, n. gen. n. sp., from Kpogamé-Hahotoé. All specimens are shown in right lateral view. Upper teeth (from back to front): 1–4, KPG-M 4, right  $M^2$  in anterior, lingual, posterior, and lateral views; 5, KPG-M 39, left  $P^3$  (reversed); 6, KPG-M 9, left  $P^1$  (rev.); 7, KPG-M 3, possible right  $C^1$ ; 8, KPG-M 32, right  $I^3$ ; 9, KPG-M 50, right  $I^2$ ; 10, KPO-M 8, right  $I^1$ ; lower teeth (from back to front): 11, KPG-M 127, heavily worn right  $M_2$ ; 12, KPG-M 19, little worn right  $M_2$ ; 13, KPG-M 24, left  $M_1$  (rev.); 14, KPG-M 12, right  $P_2$ ; 15, KPG-M 14, possible right  $C_1$ ; 16, KPG-M 7, right  $I_2$ . Note retention of a distinct protocone cusp on  $M^2$ ; single-rooted  $P^1$ ; relatively low protoconid height on  $M_2$ , with no trace of a metaconid (Fig. 5.12); and low protoconid height on  $M_1$ , with a large and distinct metaconid just posterior to the protoconid (Fig. 5.13). Abbreviations: *hyd*=hypoconid; *mtc*=metacone; *mtd*=metaconid; *pac*=paracone; *prc*=protocone; *prd*=protoconid.

*Maiacetus inuus* (GSP-UM 3475 and 3551; Gingerich et al., 2009). Most teeth of *Togocetus* have slightly rugose enamel, and many are slightly worn, which also helped in identifying their position. Upper and lower teeth representing a partial right permanent dentition are illustrated in Figure 5. Here again, teeth known only from the left side have been reversed for consistency.

Incisors and canine teeth of protocetids are all single rooted. Here KPO-M 8 (Fig. 5.10), KPG-M 50 (Fig. 5.9), and KPG-M 32 (Fig. 5.8), interpreted as right  $I^1$ , right  $I^2$ , and right  $I^3$ , can be recognized as upper incisors by their posteriorly oriented roots. The crown of  $I^3$  is conspicuously smaller than those of  $I^1$  and  $I^2$ . KPG-M 3 (Fig. 5.7) is a large right caniniform tooth interpreted as

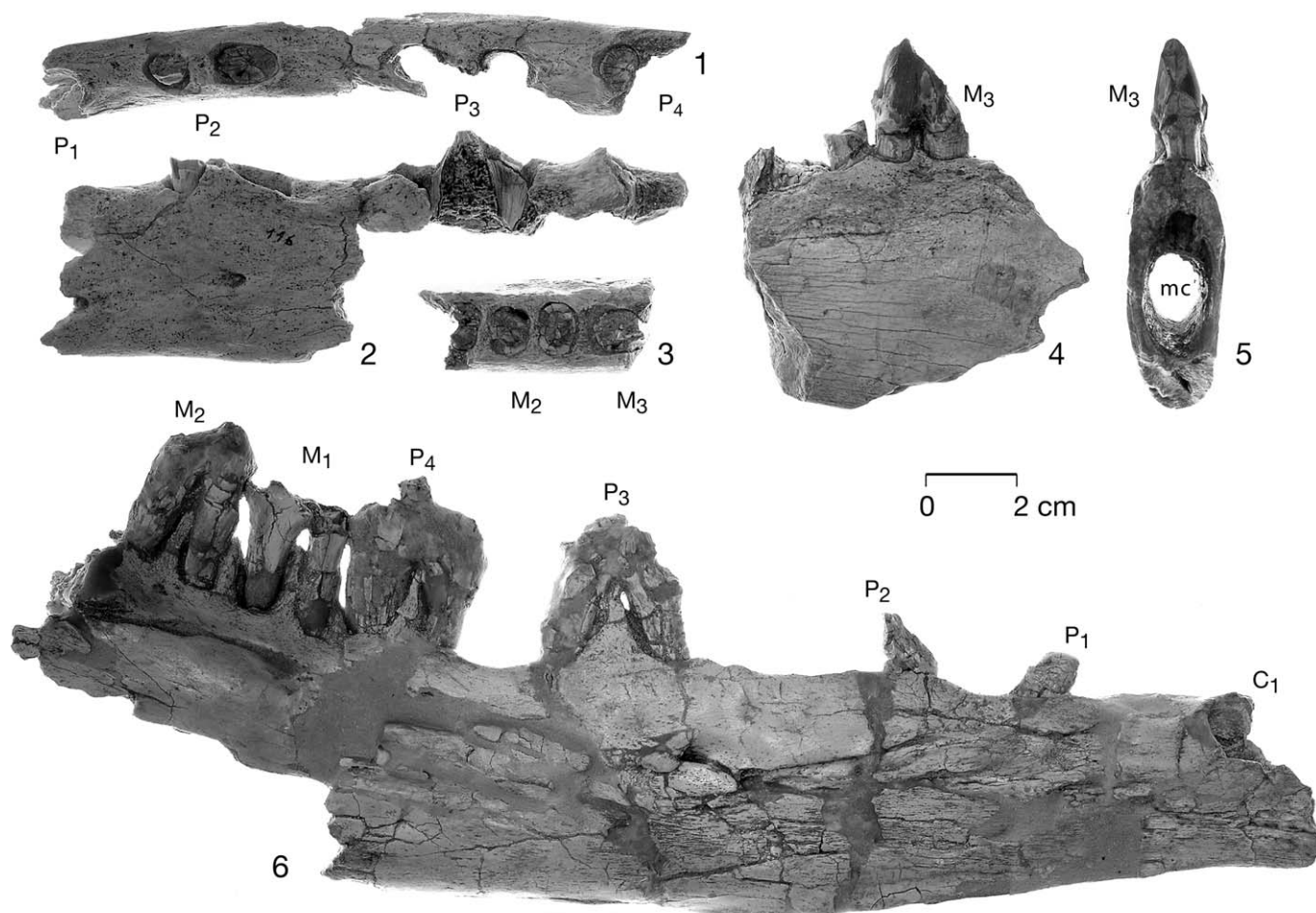


FIGURE 6—Dentary remains of middle Lutetian *Togocetus traversei*, n. gen. n. sp., from Kpogamé-Hahotoé. 1, 2, KPO-M 116, partial left dentary with roots or alveoli for a single-rooted  $P_1$  and double-rooted  $P_{2-4}$ , in occlusal and left lateral view; 3, KPG-M 68, partial right dentary with roots for  $M_{2-3}$ ; 4, 5, KPG-M 1 (holotype), partial left dentary with  $M_3$ ; 6, KPO-M 142, right dentary with the alveolus for  $C_1$ ; and partial crowns of  $P_1$ – $M_2$ . Note the narrow, deep dentaries; end of the mandibular symphysis near the anterior root of  $P_3$  (Fig. 6.1, 6.6); diastemata separating  $C_1$ ,  $P_1$ ,  $P_2$ ,  $P_3$  and  $P_4$  (Fig. 6.6); and unusually small mandibular canal for a protocetid (Fig. 6.5). Abbreviation: mc=mandibular canal.

an upper canine of *Togocetus*, however it could also be an incisor of a larger archaeocete. KPG-M 9 (Fig. 5.6) has an anteroposteriorly elongated crown but a single root, meaning it is clearly  $P^1$ . No tooth has been identified as  $P^2$ , but KPG-M 39 (Fig. 5.5) is a left  $P^3$ . This crown is interesting in having a single apical cusp (paracone), in having a distinct posterolingual swelling at the base of the crown representing some vestige of a protocone, and in having the occlusal crest anterior to the paracone extend forward but then curve lingually to join the lingual cingulum before reaching the anterior end of the crown. KPG-M 59 and KPG-M 134 (not illustrated) are partial crowns of  $P^4$  that are similar to that of  $P^3$  but have a wider protocone swelling and possibly a distinct medial root.

The only tooth identifiable as  $M^1$  is KPG-M 131, which preserves the paracone and metacone and little else. It is much lower crowned than  $M^2$  or  $M^3$ . KPG-M 4 (Fig. 5.1–5.4) is a right  $M^2$ , and this is the best preserved of the upper cheek teeth. It has a prominent paracone, a slightly smaller metacone, and a distinct protocone on the lingual side at the base of the crown. There is a continuous crest of enamel from the basal cingulum at the anterior margin of the crown up the front of the paracone (preparacrista), down the back of the paracone, up the front of the metacone, and down the back of the metacone to the posterior basal cingulum. The preparacrista is doubled near the base of the crown, enclosing

a small shallow fovea like that on the anterior surface of some lower molars. There are anterior and posterior interproximal facets perforating the enamel, indicating that  $M^2$  was in a closely packed molar row. Enamel is perforated by wear at the apex of the protocone, along the anterior margin of the crown, and on both the anterior and posterior occlusal surfaces of the hypocone. There is a long narrow facet of polished occlusal wear connecting the apex of the paracone to the protocone.

$M^2$  is three-rooted, but the medial and posterior roots are confluent. When viewed occlusally, the anterior margin of the crown is angled at about  $45^\circ$  relative to the lateral margin, while the posterior margin is angled at about  $90^\circ$ . It is noteworthy that these margins are straight and not concave as they commonly are in other protocetids. KPG-M 6, KPG-M 28, and KPG-M 38 (not illustrated) have crowns very similar to that of KPG-M 4 and all may represent  $M^2$ . KPG-M 6 differs from KPG-M 4 in having a stronger doubled preparacrista that encloses a larger and deeper anterior fovea. If any of these teeth represents  $M^1$ , then  $M^1$  is virtually indistinguishable from  $M^2$ .  $M^3$  is seemingly not present in the available specimens of *Togocetus traversei*.

Lower incisor and canine teeth are similar to the corresponding uppers, but generally have straighter roots. KPG-M 7 (Fig. 5.16) is a right  $I_2$ , and KPG-M 14 (Fig. 5.15) is possibly a right  $C_1$ . Dentary KPO-M 142 has  $P_1$  in place in the jaw, but the crown is



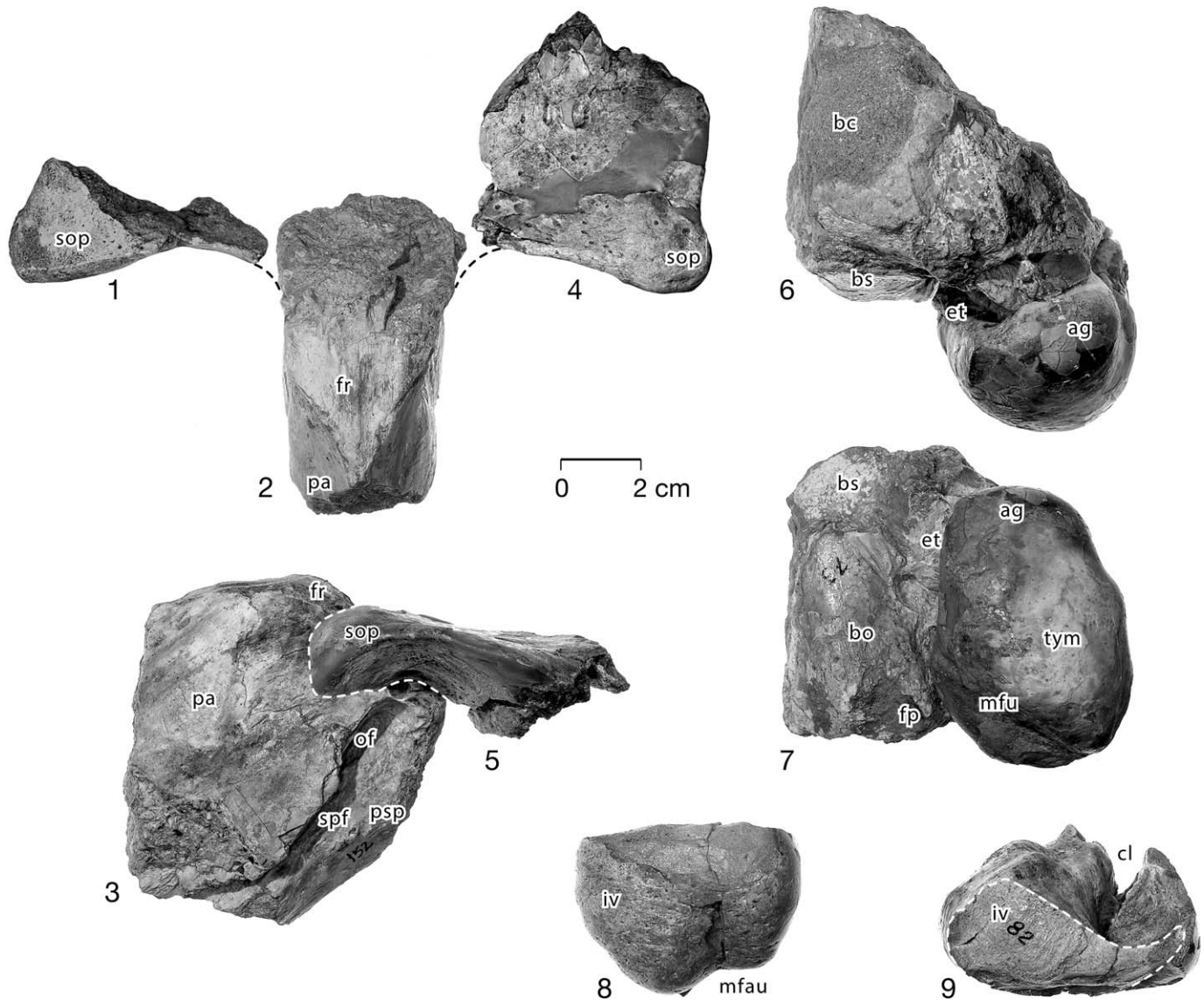


FIGURE 7—Cranial remains of middle Lutetian *Togocetus traversei*, n. gen. n. sp., from Kpogamé-Hahotoé. 1, KPG-M 146, left supraorbital portion of frontal in dorsal view; 2, 3, KPG-M 152, midcranial pons or intertemporal constriction of cranium in dorsal and right lateral views; 4, 5, KPG-M 147, right supraorbital portion of frontal in dorsal and right lateral views; 6, 7, KPG-M 73, left side of braincase and left tympanic bulla in anterior and ventral views; 8, 9, KPG-M 82, partial left tympanic bulla in ventral and anterior views. Note well-developed frontal shield characteristic of Protocetidae (Fig. 7.1, 7.4; elements separated slightly for clarity); moderate size of the tympanic bulla (Fig. 7.6, 7.7); and osteosclerosis of the tympanic bulla (Fig. 7.8, 7.9). Abbreviations: ag=anterior angle of tympanic bulla; bc=braincase (sediment filled); bs=basisphenoid; cl=posterior cleft; et=trough for eustachian tube; fp=falcate process; fr=frontal; iv=involucrum; mf=median furrow; of=orbital foramen; pa=parietal; psp=presphenoid; sop=supraorbital process; spf=sphenorbital fissure; tym=tympanic bulla.

heavily worn. KPG-M 12 (Fig. 5.14) is the crown of a double-rooted right  $P_2$ . The crown of this tooth is interesting in being conspicuously concave lingually and convex labially in both anteroposterior and dorsoventral directions. KPG-M 142 has part of the crown of  $P_2$  that shows this curvature as well. Crowns of  $P_3$  and  $P_4$  are present in KPG-M 142. These are typically the longest and most high-crowned teeth in protocetids, and that appears to be the case here as well (although neither  $P_3$  nor  $P_4$  can be measured accurately because each is poorly preserved). Enamel is present on the lingual surfaces of the crowns, but buccal surfaces of both are heavily worn.  $P_4$  retains a cusp near the posterior base of the crown.  $P_{3-4}$  are similar in comparable parts to those of other early protocetids.

One of the most distinctive teeth in the dentition of *Togocetus traversei* is  $M_1$ . The best example is KPG-M 24 (Figs. 4.7, 5.13). This is a normally proportioned protocetid molar, with robust

anterior and posterior roots. The crown has three prominent cusps: the protoconid forms the apex of the crown; this is followed by a slightly lower and smaller, confluent metaconid; and there is, finally, a substantial but much lower hypoconid. There is no trace of a paraconid on the trigonid. The three cusps are aligned almost anteroposteriorly on the crown, but the metaconid is positioned a little more lingually than the other two cusps. There is a single anterior paracristid running from the anterior cingulid to the apex of the protoconid, a short metacristid connecting the protoconid and metaconid, a longer cristid connecting the metaconid and hypoconid, and finally a short cristid connecting the hypoconid to the posterior cingulid. All four cristids are aligned anteroposteriorly. The paracristid is worn but evidently bore two or three small cusps.

KPG-M 24 has a faint cingulid surrounding the base of the  $M_1$  crown, and deep interproximal facets on the anterior and posterior

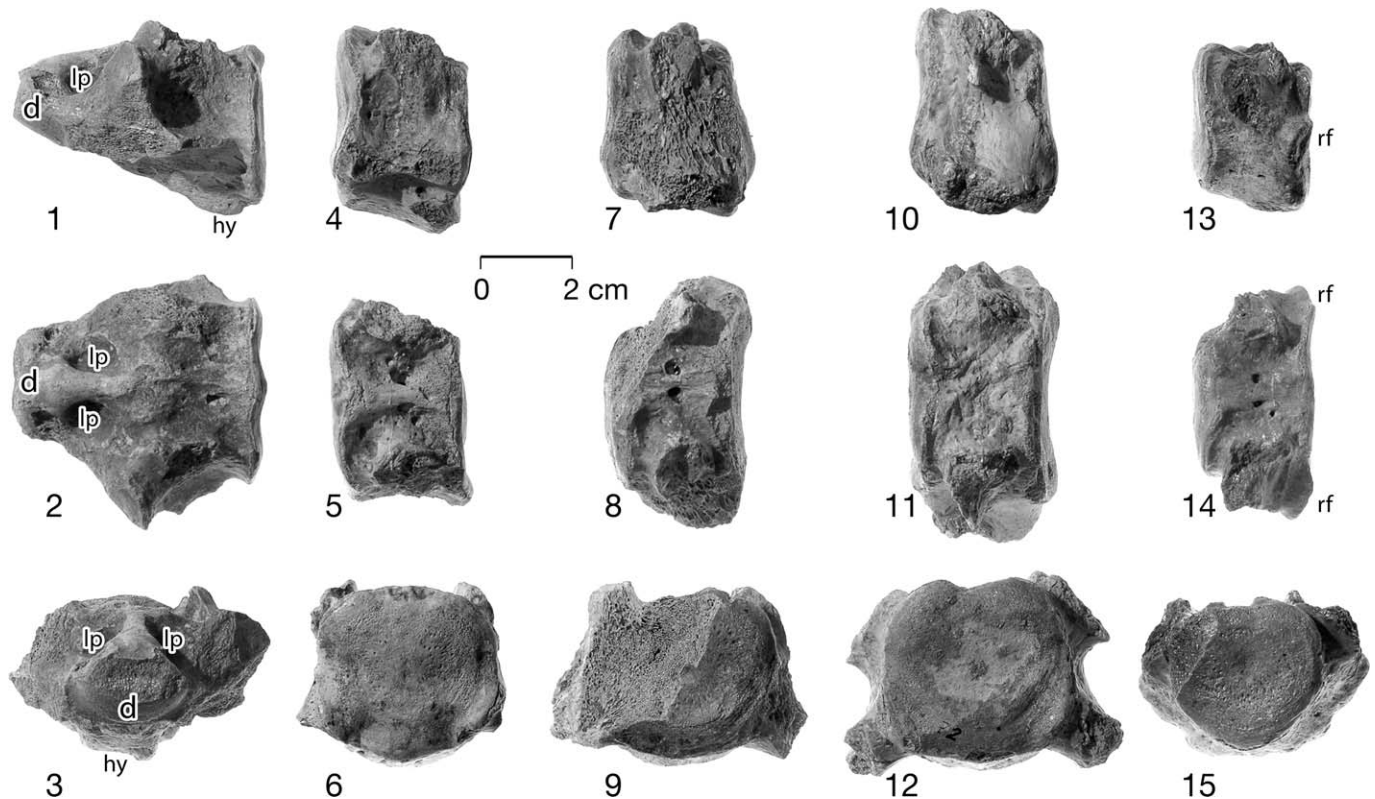


FIGURE 8—Cervical vertebrae of middle Lutetian *Togocetus traversei*, n. gen. n. sp., from Kpogamé-Hahotoé. Each vertebra is shown in left lateral, dorsal, and anterior views. 1–3, KPG-M 69, C2 vertebra (axis); note large ligamentous pits on the dorsal surface of the dens; 4–6, KPG-M 110, C4 vertebra; 7–9, KPG-M 64, C5 vertebra; 10–12, KPG-M 72, C6 vertebra; 13–15, KPG-M 102, C7 vertebra. Note relatively long centra of all cervical vertebrae, hypapophyses on C2 and C4, trapezoidal lateral profile of C4 with anterior and posterior surfaces parallel (Fig. 8.4), and wedged lateral profiles of C5 (Fig. 8.7) and C6 (Fig. 8.10). Abbreviations: *d*=dens; *hy*=hypapophysis, *lp*=ligamentous pit; *rf*=rib facet.

margins of the crown for contact with  $dP_4$  (or  $P_4$ ) and  $M_2$ , respectively. Each of the three cusps is worn slightly, with dentine showing at each apex. The buccal surface of the tooth is highly polished where it wore against  $M_1$ . KPG-M 42 is the anterior or trigonid portion of a second  $M_1$  that is a little larger than KPG-M 24, with a more worn protoconid and metaconid. KPG-M 42 has a second anterior crest, which rises from the anterobuccal base of the crown and joins the paracristid high on the protoconid. Together these enclose a distinct groove. The interproximal facet for contact with  $P_4$  is not in this groove, but well developed on the anterior cingulid itself.  $M_1$  is also present in the dentary KPO-M 142, but little can be seen except deep occlusal wear on the buccal surface of the crown, like the polished wear on KPG-M 24, but much deeper.

$M_2$  is represented by several tooth crowns. The best preserved is KPG-M 19 (Fig. 5.12). This has two cusps only, the high apical protoconid and the low posterior hypoconid. There is no trace of a metaconid. The paracristid starts at the anterolingual base of the crown and runs dorsally and posteriorly to the apex of the protoconid. The crest continues down the back of the protoconid to the notch between the two cusps, up the anterior surface of the hypoconid, and finally down the posterior surface of the hypoconid to join the basal cingulid. There is a basal cingulid encircling the crown, which is more distinct on the lingual surface and fainter on the buccal surface of the crown. The base of the crown is flat to shallowly concave anteriorly, but the anterior surface is not distinctly grooved as it is in some molars here. KPG-M 127 (Fig. 5.11) and KPG-M 130 are antimeres that are deeply worn both apically and across the posterobuccal occlusal surface of the protoconid and anterobuccal occlusal surface of the

hypoconid. Here again the interproximal facet for contact with  $M_1$  was at or below the basal cingulid. KPG-M 35, KPG-M 36, and KPG-M 37 are all very similar partial crowns of  $M_2$ . KPG-M 35 differs in having a distinct cusplule in the middle of the paracristid.  $M_2$  is present in KPO-M 142 (Fig. 6.6) but here again it is heavily worn with only the lingual surface well preserved.

The best preserved  $M_3$  is in the left dentary KPG-M 1. The crown is damaged but shows that the crown of  $M_3$  was generally similar to that of  $M_2$ . Bone present posterior to this tooth shows that it is clearly a last lower molar, which in archaeocetes is  $M_3$ . KPG-M 128 is another  $M_3$ , seemingly associated with  $M_2$ s KPG-M 127 and KPG-M 130, with a heavily worn protoconid that is not quite as worn as that on the two  $M_2$ s; it is otherwise similar to  $M_2$  in form. KPG-M 41 is the anterior half of a molar that could be  $M_2$  or  $M_3$ .

Measurements of all permanent teeth are included in Table 1.

**Dentaries.**—Parts of two left dentaries and two right dentaries are known for *Togocetus traversei* (Fig. 6), and similar preservation suggests that one left and one right dentary may belong to the same individual. KPO-M 116 is a well preserved left dentary with an alveolus for  $P_1$ , roots for a double-rooted  $P_2$ , and alveoli for  $P_3$  and  $P_4$  (Fig. 6.1, 6.2). The diastema between  $P_1$  and  $P_2$  is 15.0, that between  $P_2$  and  $P_3$  is 23.8, and that between  $P_3$  and  $P_4$  is 13.1 mm. The medial surface of the dentary anterior to  $P_3$  is textured like a normal mandibular symphysis, indicating that left and right dentaries were unfused. The dentary is unusually narrow and deep, measuring 15.9 mm wide and 43.6 mm deep in cross-section at  $P_2$ . In life, with left and right dentaries articulating, the mandible was still notably narrower than deep. KPG-M 68 includes pieces of a right dentary that match KPO-M

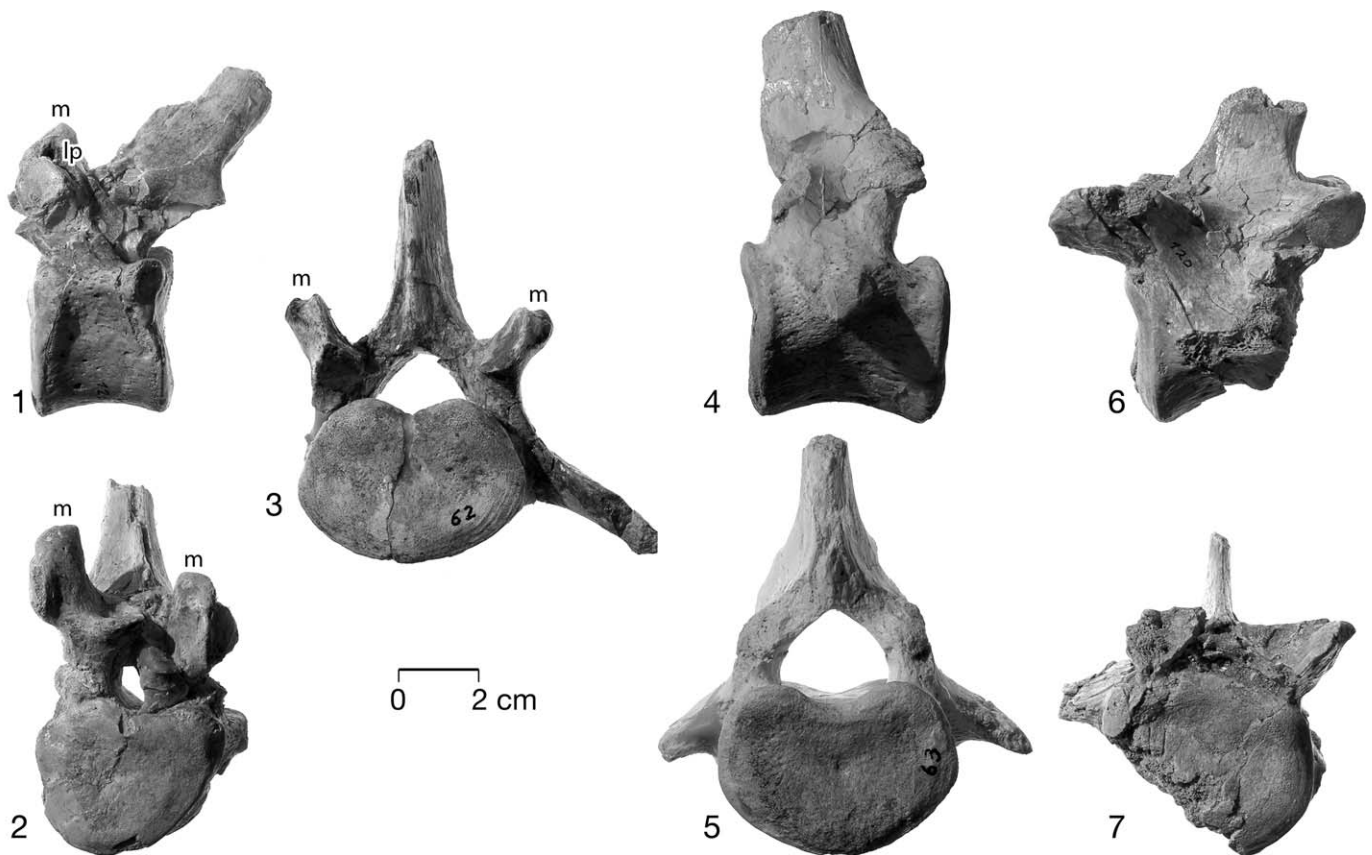


FIGURE 9—Thoracic, lumbar, and caudal vertebrae of middle Lutetian *Togocetus traversei*, n. gen. n. sp., from Kpogamé-Hahotoé. 1–2, KPG-M 125, thoracic T5 vertebra in left lateral and anterior views; note large ligamentous pit on the posterolateral surface of the metapophysis; 3, KPG-M 62, lumbar L4 vertebra in anterior view; 4, 5, KPG-M 63, lumbar L6 vertebra in left lateral and anterior views. 6, 7, KPG-M 120, caudal Ca2 vertebra in left lateral and anterior views. Identifications of thoracic, lumbar, and caudal vertebrae are approximate because the complete series of *Togocetus traversei* is not known. Abbreviations: *lp*=ligamentous pit; *m*=metapophysis.

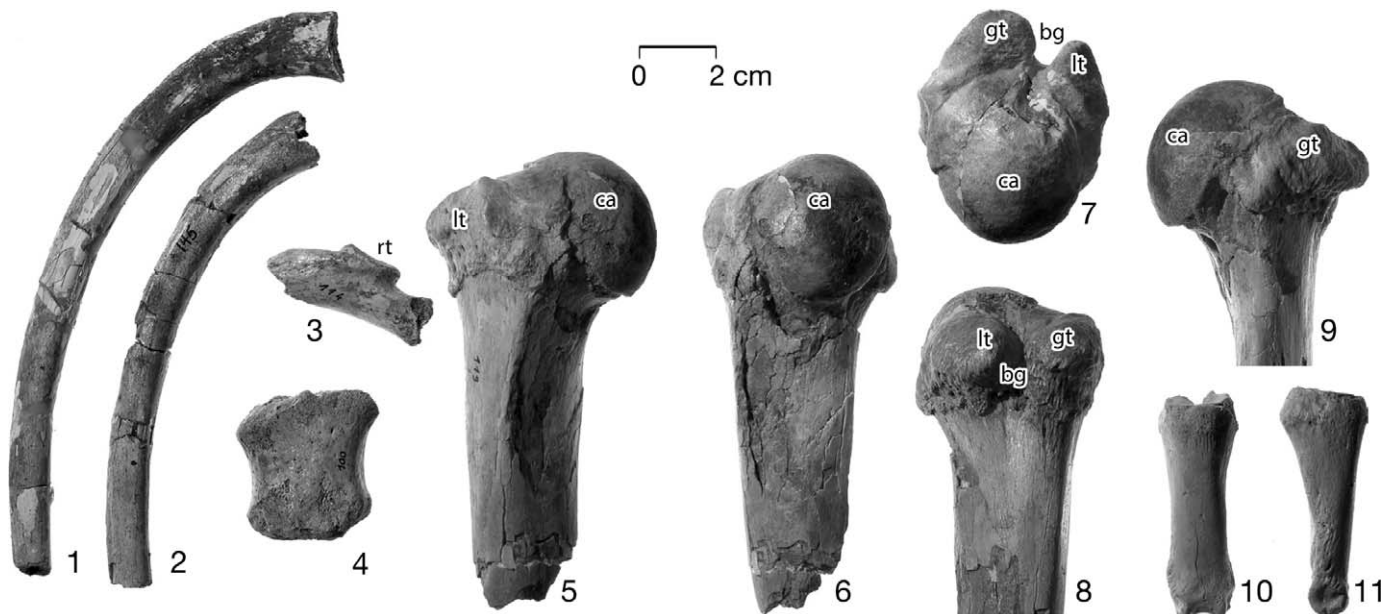


FIGURE 10—Rib pieces, sternebra, humerus, and manual phalanx of middle Lutetian *Togocetus traversei*, n. gen. n. sp., from Kpogamé-Hahotoé. 1, KPG-M 143, dorsal half of the body of a right rib in anterior view; 2, KPG-M 145, dorsal half of the body of a right rib in anterior view; 3, KPG-M 114, proximal end of a right rib with the capitulum and tuberculum (capitulum missing the proximal epiphysis); 4, KPG-M 100, midline second sternebra in anterior view; 5–9, KPG-M 119, proximal half of a left humerus in lateral, posterior, proximal, anterior, and medial views; note the hemiovoid head on the humerus, and the large greater and lesser tubercles flanking a deep bicipital groove; 10, 11, KPG-M 67, manual phalanx III-1 of the right hand in dorsal and lateral views. Abbreviations: *bg*=bicipital groove; *ca*=caput or head; *gt*=greater tubercle; *lt*=lesser tubercle; *rt*=rib tubercle.

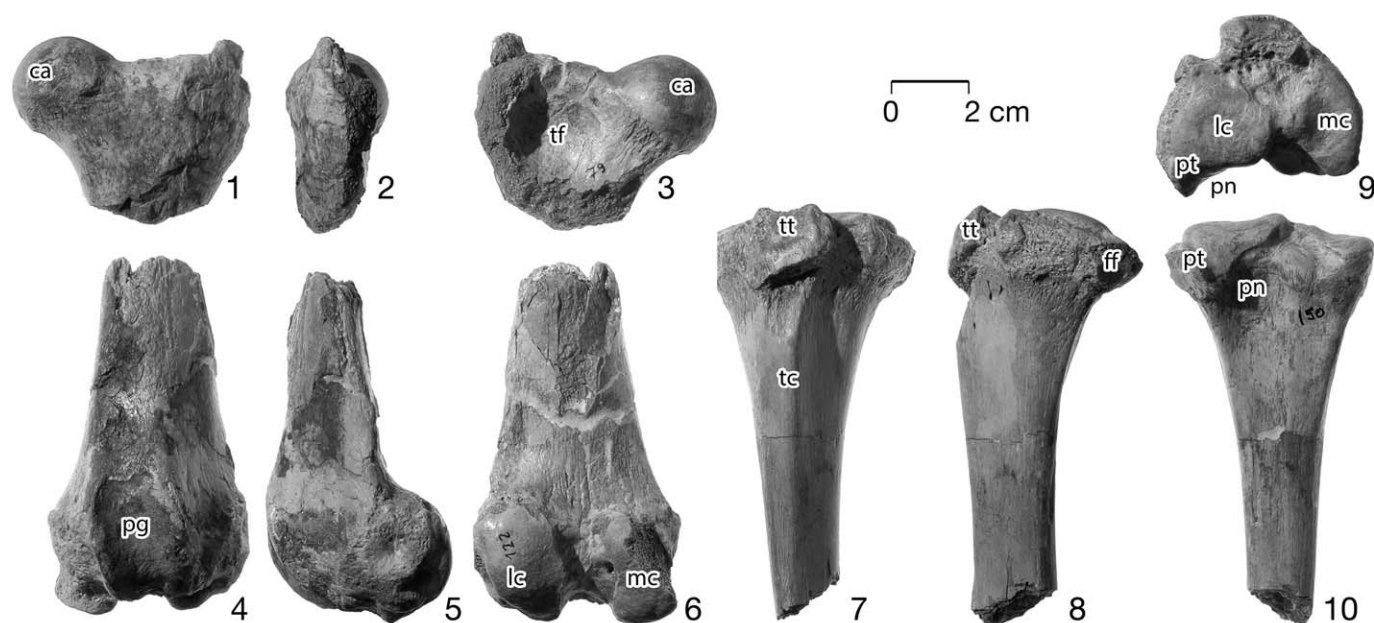


FIGURE 11—Hind limb elements of middle Lutetian *Togocetus traversei*, n. gen. n. sp., from Kpogamé-Hahotoé. 1–3, KPG-M 79, proximal end of a left femur in anterior, lateral, and posterior views; 4–6, KPG-M 122, distal half of a left femur in anterior, lateral, and posterior views; 7–10, KPG-M 150, proximal end of a left tibia in anterior, lateral, proximal, and posterior views. These three elements are possibly all parts of the same hind limb. Note absence of a fovea on the femoral head, broad distal femur, angulation of the patellar groove and femoral condyles on the femur, and the deep groove for the flexor digitorum longus tendon on the tibia. Abbreviations: ca=caput or head; ff=fibular facet; mc=medial condyle; lc=lateral condyle; pg=patellar groove; pn=popliteal notch; pt=popliteal tuberosity; tc=tibial crest; tf=trochanteric fossa; tt=tibial tuberosity.

116 in preservation. The most complete piece has roots for  $M_{2-3}$  (Fig. 6.3).

The most interesting mandibular specimen is KPG-M 1, the left dentary of the holotype of *Togocetus traversei* (Fig. 6.4, 6.5). This has roots for  $M_2$  and the crown of  $M_3$  in place. It is proportioned more normally, with a cross section below  $M_2$  measuring 22.8 mm wide and 55.2 deep. What is most distinctive is the very small mandibular canal, which is only 14.3 mm wide and 22.3 mm deep measured below the posterior root of  $M_3$  (see below for discussion; as mentioned above, bone present posterior to this tooth shows that it is clearly a last lower molar, which in archaeocetes is  $M_3$ ).

KPO-M 142 is the most complete of the dentaries (Fig. 6.6), running from the alveolus for  $C_1$  to the crown of  $M_2$ , and measuring 28.5 cm in length as preserved. It is reasonably well preserved, resembling KPO-M 116 anteriorly and KPG-M 1 posteriorly, but all of the teeth are heavily worn. The lingual surfaces of the posterior cheek teeth still bear enamel, but the buccal surfaces are heavily worn. The crown of  $M_1$  is about one-half as wide as it was initially, with the other half of the tooth having been removed by occlusal wear. The diastema between  $C_1$

and  $P_1$  measures 31.0, that between  $P_1$  and  $P_2$  is 16.9, that between  $P_2$  and  $P_3$  is 21.9, and that between  $P_3$  and  $P_4$  is 16.9 mm. There are no diastemata between teeth posterior to  $P_4$ . The medial surface of the dentary anterior to the anterior root of  $P_3$  is textured like a normal mandibular symphysis, again indicating that left and right dentaries were unfused. Here the dentary is narrow and deep anteriorly, measuring 16.2 mm wide and 53.6 mm deep in cross-section at  $P_2$ . As before, in life, with left and right dentaries articulating, the mandible was notably narrower than deep. It is not possible to measure the size of the mandibular canal below  $M_3$  in KPO-M 142, but the canal was clearly small like that of KPG-M 1 and not excavated as close to the roots of  $M_3$  as it is in other protocetids.

**Cranial elements.**—The cranium of an archaeocete can be divided into an anterior facial part and a posterior braincase part, connected by an intervening frontoparietal-presphenoid mass of bone called the midcranial pons. The cranium of *Togocetus traversei* is represented by portions of the midcranial pons, the frontal shield, two squamosals, and a portion of a braincase with a tympanic bulla.

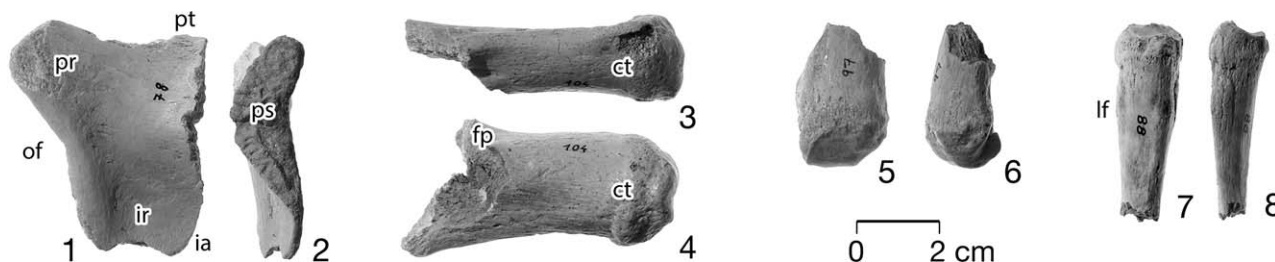


FIGURE 12—Hind limb elements of middle Lutetian *Togocetus traversei*, n. gen. n. sp., from Kpogamé-Hahotoé. 1, 2, KPO-M 78, pubic portion of a left innominate; 3, 4, KPO-M 104, body of a right calcaneum; 5, 6, KPG-M 97, distal end of a left metatarsal IV; 7, 8, KPG-M 88, proximal portion of a right middle phalanx of a fourth toe (right IV-2). Abbreviations: ct=calcaneal tuber; fp=fibular process; ia=ischial arch; ir=ischial ramus; lf=lateral flange; of=obturator foramen; pr=pubic ramus; ps=pubic symphysis; pt=pubic tubercle.

TABLE 1.—Dental remains of *Togocetus traversei*, n. gen. n. sp., from Kpogamé-Hahotoé. Length is recorded as the maximum anteroposterior diameter of the tooth crown, width is the maximum buccal-lingual diameter, and height is the vertical distance from the base of the crown to the tip. Abbreviations: C=canine; I=incisor; M=molar; P=premolar. Measurements are in mm.

Specimen	Position and description	Length	Width	Height	Figure
KPG-M 1	Left dentary with M <sub>3</sub> (holotype)	21.0	13.2	—	Fig. 6.4, 6.5
KPG-M 3	Right C <sup>1</sup> (?)	21.9	13.6	—	Fig. 5.7
KPG-M 4	Right M <sup>2</sup>	21.4	20.6	20.1	Fig. 5.1–5.4
KPO-M 5	Incisor or canine	18.9	11.3	—	—
KPG-M 6	Right M <sup>2</sup>	23.5	19.2	19.8	—
KPG-M 7	Right I <sub>2</sub> (?)	17.9	10.8	22.8	Fig. 5.16
KPO-M 8	Right I <sup>1</sup> (?)	16.0	10.0	—	Fig. 5.10
KPG-M 9	Left P <sup>1</sup> (single-rooted)	17.5	8.6	14.6	Fig. 5.6
KPG-M 10	Left dP <sup>4</sup>	26.0	13.4	16.0	Fig. 4.1
KPG-M 11	Left dI <sup>1</sup> (single-rooted)	11.8	7.5	13.4	Fig. 4.6
KPG-M 12	Right P <sub>2</sub> (double root, robust)	24.8	10.8	22.6	Fig. 5.14
KPG-M 13	Incisor or canine	18.5	13.3	—	—
KPG-M 14	Right C <sub>1</sub> (?)	19.7	12.4	32.8	Fig. 5.15
KPG-M 15	Left dP <sub>3</sub> (double-rooted)	24.0	7.9	16.4	Fig. 4.9
KPG-M 16	Right dP <sub>2</sub> (double-rooted)	18.8	6.6	13.1	Fig. 4.10
KPG-M 17	Incisor or canine	21.1	14.0	—	—
KPG-M 18	Incisor or canine	21.3	11.0	—	—
KPG-M 19	Right M <sub>2</sub>	25.6	11.6	23.1	Fig. 5.12
KPG-M 20	Right P <sup>1</sup> (single-rooted)	17.5	8.4	—	—
KPG-M 21	Right I <sup>2</sup>	9.9	8.1	—	—
KPG-M 22	Right I <sup>3</sup>	14.2	10.1	—	—
KPG-M 23	Left dP <sub>4</sub>	35.0	10.2	—	Fig. 4.8
KPG-M 24	Left M <sub>1</sub>	25.2	11.8	20.0	Figs. 4.7, 5.13
KPG-M 25	Right dC <sub>1</sub>	13.0	8.6	17.0	Fig. 4.11
KPG-M 26	Left I <sup>2</sup> (?)	21.5	12.0	24.8	—
KPG-M 27	Right dC <sup>1</sup>	14.1	8.8	18.8	Fig. 4.3
KPG-M 28	Right M <sup>2</sup> (?)	22.3	20.8	—	—
KPG-M 29	Right dI <sup>1</sup> (?)	13.4	7.8	—	Fig. 4.5
KPG-M 30	Right dI <sup>3</sup>	6.3	5.0	7.8	Fig. 4.4
KPG-M 31	Premolar, part (worn)	—	10.3	—	—
KPG-M 32	Right I <sup>3</sup>	13.7	9.4	—	Fig. 5.8
KPG-M 34	Incisor	19.8	10.4	23.7	—
KPG-M 35	Right M <sub>2</sub> (high-crowned, but lower than <i>Rodhocetus</i> )	—	13.8	26.3	—
KPG-M 36	Right M <sub>3</sub> (high-crowned)	—	13.0	22.5	—
KPG-M 37	Left M <sub>2</sub> (high-crowned)	—	13.4	25.7	—
KPG-M 38	Left M <sub>2</sub> (?)	19.8	20.8	—	—
KPG-M 39	Left P <sup>3</sup>	—	—	21.7	Fig. 5.5
KPG-M 40	Incisor or canine	23.3	15.8	—	—
KPG-M 41	Left M <sub>2</sub> or M <sub>3</sub>	—	11.2	22.0	—
KPG-M 42	Left M <sub>1</sub>	—	13.2	22.0	—
KPG-M 43	Left I <sup>3</sup>	—	8.9	—	—
KPG-M 44	Incisor or canine	14.8	9.1	13.1	—
KPG-M 45	Incisor or canine	12.5	9.4	—	—
KPG-M 46	Premolar	—	10.5	—	—
KPG-M 47	Incisor or canine	15.1	10.7	—	—
KPG-M 48	Incisor or canine	10.4	8.4	—	—
KPG-M 49	Premolar, part	—	11.8	—	—
KPG-M 50	Incisor or canine	13.4	10.8	—	—
KPG-M 51	Incisor or canine	21.7	13.1	—	—
KPO-M 52	Left P <sup>2</sup> , posterior half (gracile)	—	9.1	—	—
KPG-M 53	Incisor or canine	17.6	10.3	—	—
KPG-M 54	Right M <sup>2</sup> , part	—	—	17.8	—
KPG-M 55	Incisor or canine	19.8	11.2	—	—
KPG-M 56	Premolar, part	—	8.1	—	—
KPG-M 57	Premolar, part	—	9.3	—	—
KPG-M 58	Right dP <sup>4</sup> (posterior portion)	—	14.4	12.4	—
KPG-M 59	Left P <sup>4</sup>	—	16.4	22.3	—
KPO-M 61	Incisor	15.3	11.4	—	—
KPG-M 126	Right P <sup>3</sup> , posterior half (gracile)	—	13.0	—	—
KPG-M 127	Right M <sub>2</sub> (antimere of KPG-M 130)	25.1	11.7	—	Fig. 5.11
KPG-M 128	Left M <sub>3</sub> (part of KPG-M 127 through KPG-M 130, less worn)	—	11.2	—	—
KPG-M 129	Right P <sub>2</sub> (posterior portion, gracile)	—	8.9	—	—
KPG-M 130	Left M <sub>2</sub> trigonid (antimere of KPG-M 127)	—	11.2	—	—
KPG-M 131	Left M <sup>1</sup> (low-crowned, large metacone)	—	—	13.5	—
KPG-M 132	Premolar <sub>3</sub> part (anterior or posterior crown)	—	13.1	—	—
KPG-M 133	Right dP <sup>3</sup>	27.3	12.0	17.4	Fig. 4.2
KPG-M 134	Left P <sup>4</sup>	—	—	21.7	—
KPG-M 135	Right M <sub>2</sub> , trigonid	—	—	—	—
KPG-M 136	Left M <sup>3</sup> (partial crown)	—	18.0	18.0	—
KPG-M 137	Incisor or canine	13.9	12.4	—	—
KPG-M 138	Incisor or canine	22.1	13.8	—	—
KPG-M 139	Incisor or canine	18.6	11.0	—	—
KPG-M 140	Incisor or canine	16.7	12.0	—	—
KPG-M 141	Left dC <sub>1</sub>	13.1	9.7	—	—
KPO-M 142	Right dentary w. P <sub>1</sub> -M <sub>2</sub> (length symphysis to front root of P <sub>3</sub> )	66.0	19.2	—	Fig. 6.6
KPO-M 142	Right M <sub>1</sub> (crown in dentary)	23.5	—	—	Fig. 6.6
KPO-M 142	Right M <sub>2</sub> (crown in dentary)	—	10.6	—	Fig. 6.6



TABLE 2—Tympanic bullae of *Togocetus traversei*, n. gen. n. sp., from Kpogamé-Hahotoé in Togo. Measurements are in mm, with adults highlighted in bold. Differences in adult size (width) are interpreted as sexual dimorphism.

Specimen	Side	Length	Width	Depth	Age	Sex	Figure
KPG-M 33	Left	—	41.4	—	Juvenile	Male?	—
KPG-M 73	Left	<b>56.1</b>	<b>38.8</b>	<b>33.8</b>	Adult	Female	Fig. 7.6, 7.7
KPG-M 82	Left	—	<b>48.5</b>	—	Adult	Male	Fig. 7.8, 7.9
KPG-M 89	Left	—	38.6	—	Subadult	Female	—
KPG-M 93	Left	—	—	—	Adult	—	—
KPG-M 105	Left	—	<b>49.1</b>	—	Adult	Male	—
KPG-M 158	Left	—	—	—	Adult	—	—
KPG-M 80	Right	—	—	—	Adult	—	—
KPG-M 123	Right	—	<b>47.7</b>	—	Adult	Male	—
KPG-M 124	Right	—	—	—	Adult	—	—

The frontal shield was reassembled from the well-preserved pons and from supraorbital processes of the left and right frontals, all seemingly parts of the same individual. The pieces do not snap together, but they touch and they can then be aligned using their common slope and continuities of curvature. KPG-M 146 is part of the left supraorbital portion of the frontal (Fig. 7.1). KPG-M 152 is the midcranial pons or intertemporal constriction of the cranium (Fig. 7.2, 7.3). KPG-M 147 is much of the right supraorbital portion of the frontal (Fig. 7.4, 7.5). Assembled, these show that the frontal shield measured approximately 180 mm transversely from the lateral margin of one supraorbital process to the lateral margin of the other. Matrix adhering to KPG-M 152 is so similar in color and texture to bone that it is difficult to interpret most foramina that should be present in this element.

KPG-M 87 and KPG-M 90 are portions of the anterior processes of two different right squamosals. KPG-M 87 shows that the glenoid fossa of the squamosal was broad, open, and relatively short anteroposteriorly, allowing the mandibular condyle a maximum of about 25 mm of motion from front to back.

KPG-M 73 is a portion of the left side of a sediment-filled braincase with the left tympanic bulla articulated in life position (Fig. 7.6, 7.7). Unfortunately the sigmoid process and a portion of the posterolateral surface of the bulla are broken away. The tympanic articulated with a broad bullar process (later to become falciform in shape) of the squamosal anterolaterally, with the falcate process of the basioccipital posteromedially, and in life with the posterior process of the periotic (but the posterior processes of both the tympanic and periotic are missing here). There is a substantial opening between the basisphenoid and anteromedial portion of the tympanic for passage of the eustachian tube. There is also a distinct 5-mm-wide indentation

or notch in the basicranium at about the point where the basisphenoid met the basioccipital (no suture remains to mark the contact of these bones). This is possibly related to incipient development of a pterygoid sinus.

The tympanic bulla of KPG-M 73 measures 56.1 mm in anteroposterior length, 38.8 mm in width measured perpendicular to the planar lateral surface of the bulla, and 33.8 mm in depth dorsoventrally. KPG-M 82 (Fig. 7.8, 7.9) is a second tympanic bulla that is larger than that of KPG-M 73. KPG-M 82 is broken, showing the thickness and density of the involucrum. KPG-M 82 measures 48.5 mm in width, and the involucrum is 28.7 mm thick at its thickest point. For comparison, the medial wall of KPG-M 82 is only 4.2 mm thick. The posterior cleft in this specimen (Fig. 7.9) is not well enough preserved to say whether it is an exit for the posterior sinus.

Eight additional tympanic bullae of *Togocetus traversei* are present in the collection from Kpogamé. All ten are listed in Table 2, with width measurements provided when these are available. Seven of the bullae are from the left side, and three are from the right. Eight are adult bullae, with smooth, hard, dense bone; one is a subadult with some cancellous bone; and one is clearly juvenile with more cancellous bone. The bullae are bimodal in size, with modes of bulla width at 38.8 mm and 48.4 mm. The modes are interpreted as sex differences, with putative males being some 25% larger than females.

**Vertebrae.**—Seventeen vertebrae of *Togocetus traversei* can be identified to position in the vertebral column. Five are cervical vertebrae, four are thoracics, seven are lumbar, and one is a caudal. These are listed with measurements in Table 3.

The first four cervical vertebrae described here, KPG-M 69, KPG-M 110, KPG-M 64, and KPG-M 72, look like they could go together and represent a single individual animal, but the fifth, KPG-M 102, is a little smaller and clearly belonged to a different

TABLE 3—Vertebral remains of *Togocetus traversei*, n. gen. n. sp., from Kpogamé-Hahotoé. Measurements (centrum length, posterior width, and posterior height) are in mm. Anterior width and anterior height were substituted when the posterior surface of the centrum is missing.

Specimen	Position and description	Length	Width	Height	Figure
KPG-M 62	Lumbar L4 (?), anterior half of centrum and neural arch	—	56.9	41.6	Fig. 9.3
KPG-M 63	Lumbar L6 (?), nearly complete centrum with neural arch	49.2	67.1	42.3	Fig. 9.4, 9.5
KPG-M 64	Cervical C6, centrum	30.2	41.6	36.2	Fig. 8.7–8.9
KPG-M 66	Lumbar L2 (?), centrum and right lamina of neural arch	40.2	52.4	38.4	—
KPG-M 69	Cervical C2 (axis), centrum (length here without dens)	40.6	39.9	34.5	Fig. 8.1–8.3
KPG-M 71	Lumbar, transverse process	—	—	—	—
KPG-M 72	Cervical C5 (?), centrum	30.8	45.5	39.9	Fig. 8.10–8.12
KPG-M 74	Thoracic T13 (?), neural spine (post-diaphragmatic, post-anticlinal)	—	—	—	—
KPG-M 77	Lumbar, neural arch (post-diaphragmatic)	—	—	—	—
KPG-M 102	Cervical C7 centrum (rib facets on posterior surface)	25.5	50.2	31.7	Fig. 8.13–8.15
KPG-M 106	Thoracic T10 (?), centrum	48.0	52.1	36.9	—
KPG-M 110	Cervical C5, centrum	27.8	39.5	35.0	Fig. 8.4–8.6
KPG-M 115	Lumbar L3 (?), centrum (posterior half of centrum only)	—	59.5	40.8	—
KPG-M 118	Thoracic T8 (?), centrum	39.0	54.8	34.2	—
KPG-M 120	Caudal Ca2, nearly complete vertebra with neural arch	43.7	56.1	44.6	Fig. 9.6, 9.7
KPG-M 125	Thoracic T5 (?), nearly complete vertebra with neural arch	36.7	46.9	37.4	Fig. 9.1, 9.2
KPG-M 154	Lumbar L4 (?), centrum (posterior half of centrum only)	—	56.1	39.7	—



individual. All are represented by centra only, and the neural arches are missing on all.

KPG-M 69 is the centrum of an axis (C2; Fig. 8.1–8.3). The body and dens together measured approximately 55 mm in length in life (a small part of the dens is now missing). Noteworthy features of C2 are the relatively long body, deep ligamentous pits on the dorsal surface of the centrum at the base of the dens, and a relatively broad, flat hypapophysis on the ventral surface of the centrum with distinct rugosities developed near the posterolateral corners of the hypapophysis.

KPG-M 110 is the centrum of a fourth cervical vertebra (C4; Fig. 8.4–8.6). This centrum is relatively long compared to later protocetid and basilosaurid cervical centra. It is trapezoidal in lateral profile, with the anterior and posterior articular surfaces paralleling each other. The anterior articular surface is raised relative to the posterior surface. The ventral surface of the centrum has a very broad, shallow hypapophysis. There are paired nutrient foramina lateral to a midline torus on the dorsal surface of the centrum, and scattered nutrient foramina on the ventral surface.

KPG-M 64 is a centrum interpreted as that of C5 (Fig. 8.7–8.9). KPG-M 64 resembles KPG-M 110 closely, but in addition to having the anterior articular surface raised relative to the posterior articular surface, the centrum is wedge-shaped, with anterior and posterior surfaces converging dorsally rather than being parallel. Bases of the transverse processes show that the transverse processes were well developed on C5.

KPG-M 72 is a centrum of C6 (Fig. 8.10–8.12). It resembles KPG-M 64 in having the anterior articular surface raised relative to the posterior surface, and in having anterior and posterior articular surfaces that converge dorsally. Bases of the transverse processes are more robust and downwardly oriented compared to those on KPG-M 64, as is typical on C6. The dorsal surface of the centrum lacks a midline torus and lacks nutrient foramina.

KPG-M 102 is a centrum of C7 (Fig. 8.13–8.15). The length of the centrum is a little shorter than those of preceding cervicals, but there is a more conspicuous difference in the size and shape of anterior and posterior articular surfaces. The posterior surface is larger than the anterior surface and more elliptical, with rib facets at the lateral poles. There are no transverse processes. There are paired nutrient foramina on the dorsal surface of the centrum, but no midline torus separating these.

Three thoracic vertebrae of *Togocetus traversei* are known, KPG-M 125, KPG-M 118, and KPG-M 106. The centra of these vertebrae differ in size and to some extent shape, but all have smoothly curved lateral and ventral surfaces, slightly convex anterior articular surfaces, and shallowly concave posterior articular surfaces. The articular surfaces are D-shaped when viewed anteriorly or posteriorly, with the straight portion of the 'D' being the dorsal surface of the centrum, and the curved portion corresponding to the lateral and ventral surfaces. The anterior and posterior surfaces of the centrum are parallel to each other when viewed laterally. There are no paired nutrient foramina on either the dorsal or ventral surfaces of the centra.

KPG-M 125 is a nearly complete vertebra interpreted as T5 (Fig. 9.1, 9.2). The centrum is narrow and deep compared to centra of the following thoracics. There are rounded facets at the dorsolateral corners of the anterior articular surface for corresponding rib capitula, and raised facets at the dorsolateral corners of the posterior articular surfaces for following rib capitula. Pedicles of the neural arches are closer together than those on following centra because the neural canal is more oval than elliptical. Prezygapophyses, arising high on the neural arch, are flat and face dorsally. These are bordered by large vertical metapophyses that also arise high on the neural arch. The

anterolateral surface of each metapophysis bears a flat facet for articulation with the corresponding rib tuberculum, while the posterolateral surface bears a deep ligamentous pit. The neural spine is somewhat triangular at the base, with a flat surface prolonging the neural canal, and lateral surfaces converging dorsally to an anterior keel. Downward-facing postzygapophyses extend posteriorly and laterally from the base of the neural spine. The neural spine is inclined posteriorly at an angle of about 45° (135° relative to the posterior surface of the centrum).

KPG-M 118 is interpreted as a centrum of T8, and KPG-M 106 is interpreted as a centrum of T10. Both lack neural arches and spines. The two centra are similar to each other in shape, being broader and shallower than the centrum of KPG-M 125. Pedicles for the neural arches are more widely spaced than those of KPG-M 125, indicating a broader, more elliptically-shaped neural canal. KPG-M 106 is the larger and better preserved of these two thoracic centra, preserving depressions for rib capitula at each corner.

KPG-M 74 is a neural spine interpreted as that of T13, but it could also be the neural spine of an anterior lumbar vertebra. The right postzygapophysis is preserved, with a ventrolateral orientation indicating that the vertebra is post-diaphragmatic. The neural spine itself is inclined anteriorly, indicating that the vertebra is post-anticlinal.

Three of the eight lumbar vertebrae of *Togocetus traversei* are complete enough to warrant description: KPG-M 66, KPG-M 62, and KPO-M 63. All have centra that are reniform when viewed anteriorly or posteriorly, with the shallowly concave portion of the kidney shape being the dorsal surface of the centrum, and the larger convex portion corresponding to the lateral and ventral surfaces. The reniform outline of the anterior surface of the centrum is a little higher and narrower than that of the posterior surface, which is a little lower and broader. The dorsal surface of the centrum flooring the neural canal is smooth and only slightly concave upward. The anterior and posterior surfaces of the centrum are shallowly concave and parallel each other when viewed laterally.

KPG-M 66 is interpreted as L2. It has a centrum like those of preceding thoracics, but with a thin transverse process projecting laterally and slightly ventrally from the body of the centrum. The neural arch and neural spine are not preserved, but the pedicles are widely separated, supporting anteroposteriorly elongated laminae. The lamina on the right side supports an anteroposteriorly elongated prezygapophysis, which is flanked laterally by a prominent metapophysis with a ligamentous pit on its postero-medial margin. It also supports an elongated but poorly preserved postzygapophysis.

KPG-M 62 is the virtually complete anterior portion of a lumbar vertebra interpreted as L4 (Fig. 9.3). This shows the reniform outline of the anterior surface of the centrum nicely. The pedicles are less widely spaced and the neural arch is narrower than those of preceding thoracic and lumbar vertebrae. The neural canal measures 23.8 mm in width near the base and 17.3 mm in height at the midline. A transverse process is preserved on the left side. This arises from the centrum and curves laterally, ventrally, and anteriorly. Large prezygapophyses arise from the laminae. These are slightly concave surfaces that face medially and slightly dorsally. They are not revolute. Metapophyses flank the prezygapophyses, but these are relatively small and lack the ligamentous pit seen on KPG-M 66. The neural spine of KPG-M 62 is inclined anteriorly about 15° relative to the anterior surface of the centrum.

KPO-M 63 (Fig. 9.4, 9.5) is similar to KPG-M 62 in comparable parts, but a little larger and more massive. KPO-M 63 is interpreted as L6. The neural arch, neural spine, and neural

canal are similar to those in KPG-M 62. The neural canal measures 26.9 mm in width near the base and 22.4 mm in height at the midline. KPO-M 63 has relatively gracile transverse processes that are angled downwardly and anteriorly, as is typical for a posteriormost lumbar vertebra.

The only caudal vertebra of *Togocetus traversei* is KPG-M 120 (Fig. 9.6, 9.7), which is interpreted as Ca2. This is crushed and deformed to some extent, but it is clear that the centrum was more cylindrical than those of preceding lumbar. Transverse processes, when present, arose from the middle of the lateral surface of the centrum. Pedicals are more closely spaced and the neural canal was narrower than those on preceding lumbar. Prezygapophyses project anteriorly beyond the anterior surface of the centrum. These are flat and face medially and dorsally. There may have been metapophyses dorsal and lateral to the prezygapophyses but nothing more than the base is preserved and this only on the left prezygapophysis. Postzygapophyses face laterally and ventrally. The neural spine is slender, short anteroposteriorly, and seemingly short dorsally, as is typical on Ca2 of protocetids.

**Rib cage.**—Several pieces of ribs are known for *Togocetus traversei*, all from the middle part of the thorax. These are curved and slender like those of other early Protocetidae, and lack both pachyostosis and osteosclerosis. The most complete is KPG-M 143 (Fig. 10.1), 16 cm long, which preserves the body of a smoothly curving right rib from the base of the tuberculum to at least the middle of the shaft. This measures 16.6 by 11.3 mm in cross section just below the tuberculum, where the exposed cortical bone is about 1 mm thick. The shaft of KPG-M 143 measures 10.8 by 10.9 mm in cross section at the distal end of the portion preserved, where the cortical bone is 2 to 3 mm thick. Even this longest piece probably represents only about one-half of the length of a whole rib.

KPG-M 145 (Fig. 10.2) is a 13 cm long portion of similar smoothly-curving right rib. This measures 15.9 by 11.9 mm in cross section just below the tuberculum, where the exposed cortical bone is 1 to 3 mm thick. The shaft of KPG-M 145 measures 11.8 by 11.0 mm in cross section at the distal end of the portion preserved, where the cortical bone is 3 to 4 mm thick.

KPO-M 114 (Fig. 10.3) is the proximal end of a third right rib with the base of the capitulum, missing its proximal epiphysis, and a well-preserved tuberculum. The tubercular facet is very shallowly saddle shaped. The body measures 14.5 by 12.0 mm in cross section just below the tuberculum. The thickness of cortical bone here appears to be about 2 mm, but this is difficult to measure accurately because of the oblique angle of the broken surface.

KPG-M 144 is an additional 13 cm long portion of a rib shaft of unknown side. This is a little larger in diameter than the other known ribs, measuring 15.8 by 9.3 mm at its proximal end and 15.3 by 11.6 mm at its distal end. Cortical bone is 2 to 3 mm thick at both ends.

The rib cage of *Togocetus traversei* is also represented by one sternebral element, KPG-M 100 (Fig. 10.4), which is probably a second sternebra. This is blocky in shape, as is typical for protocetid sternebrae. KPG-M 100 measures 40 mm in length proximodistally, 38.0 by 21.9 mm in width and thickness at one end, and 33.6 by 20.7 mm in width and thickness at the other end (it is not clear which end is proximal and which is distal). The element thins to 30.6 by 18.5 mm between the two ends.

**Forelimb elements.**—The only forelimb elements known for *Togocetus traversei* are the proximal half of a left humerus, KPG-M 119, and a complete manual phalanx, KPO-M 67.

Protocetid humeri are relatively long compared to other skeletal elements. We do not know the full length of a *Togocetus*

humerus, but comparison of KPG-M 119 (Fig. 10.5–10.9) with complete humeri of *Maiacetus inuus* (Gingerich et al., 2009) suggests that KPG-M 119 is broken at about midshaft. The head is hemiovoid and almost hemispherical, measuring 46.6 in its longer diameter and 43.3 mm in its shorter diameter. The base of the hemisphere defines a plane oriented at an angle of about 35° to the long axis of the humerus, meaning that the functional center of the head is oriented at 125° relative to the long axis (facing more posterior than dorsal). For comparison, in the basilosaurid *Dorudon atrox* the hemispheric plane is oriented at about 55° and the functional center of the head is oriented at 145° (facing more dorsal than posterior).

The greater tubercle of the KPG-M 119 humerus lies anterior to and a little below the head of the humerus, above the anterior crest of the humeral shaft. The greater tubercle is large, but only slightly larger than the lesser tubercle. The lesser tubercle lies anteromedial to and again a little below the head of the humerus. The greater and lesser tubercles flank a deep bicipital groove 5.9 mm wide and 10.7 mm deep for the biceps tendon originating from the scapular tuber adjacent to the coracoid process of the scapula. The shaft of the humerus is triangular in cross section, with the anterior crest flanked laterally by a relatively narrow surface of bone (~21 mm wide in the middle of the shaft preserved here) and medially by a broader surface of bone (~33 mm wide in the middle of the shaft preserved here). The posterior surface of the shaft here is just a little narrower than the medial surface (~32 mm wide). Oblique breakage and postmortem compression make it difficult to estimate the thickness of cortical bone in the midshaft of the humerus.

KPO-M 67 is a proximal phalanx of the middle digit of the right hand (manual phalanx III-1; Fig. 10.10, 10.11). It is closely similar to manual phalanges III-1 of *Rodhocetus balochistanensis* (GSP-UM 3485; Gingerich et al., 2001a) but differs in being shorter, straighter, more robust, and bilaterally more symmetrical. The only feature indicating that KPO-M 67 is from the right hand rather than the left is the slightly greater posterior projection of the medial portion of the proximal articular surface. Slight development of a laterally projecting flange of bone on the distal lateral surface is consistent with this. The proximal surface of KPO-M 67 for articulation with metacarpal III is circular, with a plantar notch to accommodate the sagittal keel of metacarpal III separating paired medial and lateral plantar sesamoids. Smooth surfaces flanking the plantar notch on KPO-M 67 indicate that the sesamoids articulated with the proximal plantar surfaces of phalanx III-1 as well as the distal plantar surfaces of metacarpal III. The body of phalanx III-1 tapers distally to the smoothly curved distal trochlea. The trochlea is flanked medially and laterally by ligamentous pits. The ventral surface has faint ridges of bone for insertion of flexor tendons proximal to the trochlea.

The body of KPO-M 67 is 59.4 mm long, with a proximal base measuring 21.9 mm dorsoventrally and 21.3 mm mediolaterally. The midshaft measures 11.6 mm dorsoventrally and 15.0 mm mediolaterally. The distal end of the body is 18.0 mm wide at its widest point, and the trochlea itself is 13.0 mm wide mediolaterally and 8.6 mm deep dorsoventrally.

**Hind limb elements.**—The hind limbs of *Togocetus traversei* are represented by a proximal femur, a distal femur, an isolated femoral condyle, a proximal tibia, the pubic symphysis of an innominate, a calcaneal tuber, a distal metatarsal, and a portion of a pedal phalanx.

KPG-M 79 (Fig. 11.1–11.3) is the proximal portion of a left femur possibly comprising as much as one-quarter of the total length of the bone. It is broken from the remaining shaft, meaning that the orientation of femoral head cannot be determined. The maximum width of the proximal femur, as preserved, is 64.3 mm.

The femoral head is spherical, measuring 28.5 mm in diameter. It is distinctive among protocetids in lacking a fovea capitis femoris and therefore lacking the associated ligamentum teres femoris that normally inserts in this depression. There is evidence of a prominent greater trochanter lateral to the head of the femur, but the trochanter itself is missing. A rounded bridge of bone about 18 mm long and 16.0 mm wide connected the greater trochanter to the head. On the posterior surface of the femur below this bridge there is a large trochanteric fossa. The lateral margin of this is missing, so it is impossible to judge how deep the fossa was in life. Some protocetid femora have a trochanteric fossa excavated so deeply that the bone anterolateral to the fossa is thin, but this is not the case in KPG-M 79 where the bone anterolateral to the trochanteric fossa is 8.6 mm thick. There was probably a prominent lesser trochanter too, but this portion of the femur is missing.

KPG-M 122 (Fig. 11.4–11.6) is the distal portion of a left femur possibly comprising as much as one-half of the total length of the bone. KPG-M 122 may be the distal half of the proximal femur KPG-M 79 just described. It is impossible to determine the length of the femur or whether there was any torsion of proximal and distal ends. The portion preserved is about 96 mm long. The proximal end of KPG-M 122 measures about 21.4 by 28.9 mm in diameter, which can be taken to approximate the diameter of the midshaft of a whole femur. The distal end of KPG-M 122 measures 54.6 mm in maximum breadth, which is almost twice the width at midshaft. The lateral tori of the patellar trochlea or groove are raised 50.4 mm above posterior surfaces of the femoral condyles, and the patellar groove itself is angled toward the lateral condyle distally. Salient features of the patellar trochlea are its breadth (24.5 mm), shallowness (2.7 mm), and lateral angulation (10°), and its relatively high and anterior position on the distal femur. The lateral femoral condyle is substantially larger (35.4 × 19.6 mm) than the medial condyle (31.9 × 18.1 mm). Both are relatively flat compared to other protocetids, and face posteriorly relative to the femoral shaft as is typical for protocetids. The articular surface of the lateral condyle is angled proximolaterally to mediolaterally relative to the femoral shaft, making the lateral condyle concentric about the proximal part of the lateral condyle, which is the most raised portion of the lateral condyle. A compressed indentation on the anterior surface of KPG-M 122 appears to be a bite mark but the possible predator is unknown.

KPG-M 81 is the medial condyle of a right femur that measures 33.7 × 18.5 mm, slightly larger than that of KPG-M 122.

KPG-M 150 (Fig. 11.7–11.10) is the proximal portion of a left tibia. As preserved, it measures 111.2 mm in length, and the whole tibia was probably at least twice as long. The proximal tibia measures 47.1 mm anteroposteriorly and 56.1 mm mediolaterally. The proximal end of the bone is a relatively flat table with a large lateral condyle and a smaller medial condyle. Both condyles are circular. The lateral condyle measures 28.5 mm in diameter, and the depressed center of the medial condyle measures 18.5 mm in diameter. The tibial tuberosity is large but projects little anteriorly. The tibial tuberosity, posterolateral extension of the lateral condyle, and posteromedial extension of the medial condyle define three poles of the proximal surface. Each pole is represented more distally by tibial crests: the tibial crest proper on the anterior surface of the proximal tibia, the lateral proximal crest on the posterolateral surface of the bone, and the medial proximal crest on the posteromedial surface of the bone.

There is a deep groove in the anterolateral surface of tibia KPG-M 150, lateral to the tibial tuberosity and directly anterior to the lateral condyle. This groove, reminiscent of the bicipital

groove in the humerus, constrained a large flexor digitorum longus tendon arising from the anterior part of the lateral epicondyle of the femur. Directly posterior to the lateral condyle is a posterior projection, the popliteal tuberosity, with a broad shallow groove for the proximal popliteus tendon arising from the posterior part of the lateral epicondyle of the femur. This tendon and muscle continued through the popliteal notch in the posterior margin of the proximal tibia to insert across the concavity formed on the posterior surface of the tibia between the lateral and medial proximal crests. The breadth of the proximal tibia gave the popliteus muscle substantial leverage in twisting the tibia relative to the femur. There is a circular flat facet 10.2 mm in diameter on the posterolateral surface of the popliteal tuberosity for articulation with the head of the fibula. The angle formed by posterior projections of the lateral and medial condyles of the proximal tibia was partially filled by a lower shelf of bone medial to the popliteal notch.

Both lateral and medial proximal crests of tibia KPG-M 150 merge into a rounded shaft, but the anterior tibial crest continued past the broken portion of the bone. At the distal end of the bone, near what was originally the midshaft, the tibial shaft measures 23.4 mm anteroposteriorly and 18.6 mm mediolaterally. The medullary cavity of the midshaft is an opening that measures 10.0 mm anteroposteriorly and 7.5 mm mediolaterally, with little or no cancellous bone in the medullary cavity itself. The cortical bone at this point is 9.3 mm thick anterior to the medullary cavity and 5 to 6 mm thick elsewhere. The tibial tuberosity has a sharp cutmark through its base that was almost certainly made by mining equipment.

KPO-M 78 (Fig. 12.1, 12.2) is a piece of the pubic portion of a left innominate that matches the left pubis of *Rodhocetus kasranii* (GSP-UM 3012; Gingerich et al., 2004) very closely, and mirrors the right pubis of *Maiacetus inuus* (GSP-UM 3551; Gingerich et al., 2009). As in these taxa, the KPO-M 78 pubic symphysis is arched dorsally and rugose where it articulated with its right counterpart. The symphysis is 43.8 mm long anteroposteriorly, 10 mm high where it ends anteriorly at a thickened and rounded pubic tubercle, and 2.5 mm high where it ends posteriorly in an acutely narrow ischiatic arch. This is the point where the left ischial ramus diverged from its right counterpart. There is a smooth edge of bone opposite the pubic symphysis marking the border of the obturator foramen. The pubic ramus anterior to this is 19.8 mm wide and 8.0 mm thick where it is broken. The ischial ramus posterior to this is 23.1 mm wide and only 3.3 to 4.2 mm thick where it is broken.

KPO-M 104 (Fig. 12.3, 12.4) is the long, straight, massive body of a right calcaneum. This is concave laterally and convex medially. The calcaneal tuber has a smoothly convex posterior surface for insertion of achilles tendons of the biceps femoris and gastrocnemius muscles that extend the lower leg and foot. The body of the calcaneum is broken obliquely from the posterior extremity of the fibular process dorsally to the plantar extremity of the cuboid facet ventrally. The length of the calcaneal tuber posterior to the fibular process, 55.7 mm, is closely similar to that of *Rodhocetus balochistanensis* (UM-GSP 3485). The posterior end of the calcaneal tuber measures 29.3 mm dorsoventrally and 21.3 mm mediolaterally.

KPG-M 97 (Fig. 12.5, 12.6) is the distal end of a left metatarsal IV. The fourth metatarsal is the largest and longest metatarsal in *Rodhocetus balochistanensis* (UM-GSP 3485). Little can be said about KPG-M 97 beyond noting that the articular surface for proximal phalanx IV-1 is on the dorsolateral portion of the distal end, consistent with divergence of the metatarsals and tarsal phalanges distally. The sagittal keel is prominent on the plantar surface where it separated articular surfaces for the medial and

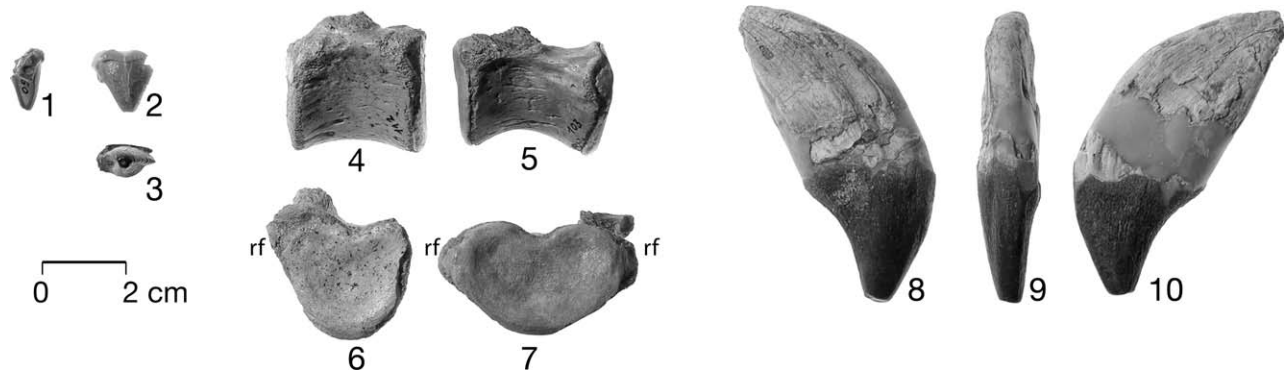


FIGURE 13—Small and large species of indeterminate protocetid archaeocetes from Kpogamé-Hahotoé. 1–3, KPG-M 60, buccal half of the left  $M^3$  of an indeterminate small protocetid, in anterior, buccal, and occlusal views; specimens are shown at the same scale as other elements here to emphasize their small size; 4, 5, TR, 112, centrum of an anterior thoracic vertebra of an indeterminate small protocetid, in left lateral and posterior views; 6, 7, KPG-M 103, centrum of a posterior thoracic vertebra of an indeterminate small protocetid, in left lateral and posterior views; 8–10, KPG-M 2, right upper canine ( $C^1$ ) of an indeterminate large protocetid, in labial, anterior, and lingual views. Abbreviation: rf=rib facet.

lateral plantar sesamoids. Proximal to the keel there is a large shallow depression, and medial to this depression there is a conspicuous flat surface. The depression and flat surface are presumably related to the development of intrinsic ligaments and muscles controlling the foot during swimming. KPG-M 97 measures 23.8 mm wide mediolaterally and 17.4 mm deep dorsoventrally at its distal end.

KPG-M 88 (Fig. 12.7, 12.8) is very similar to the right middle phalanx of the fourth toe (IV-2) in *Rodhocetus balochistanensis* (UM-GSP 3485). It is closely similar in size, with a similarly concave proximal articular surface and similarly flattened body. The body has a prominent flange of bone flanking its lateral surface that is presumably related to webbing of the phalanges. The distal end of KPG-M 88 is missing. The bone as preserved is 49.9 mm long, and the base measures 17.2 mm mediolaterally and 14.4 mm dorsoventrally. The body measures 10.3 mm mediolaterally and 6.7 mm dorsoventrally where it is broken distally.

**Remarks.**—*Togocetus traversei* is the most interesting taxon described in this study and further comments are deferred to a general discussion at the end.

#### Protocetid indeterminate (small)

**Referred specimens.**—Tooth KPG-M 60, and vertebrae KPG-M 103 and KPO-M 112 from Kpogamé, Togo.

**Description.**—KPG-M 60 (Fig. 13.1–13.3) is the buccal portion of the crown of a small left  $M^3$ . The length of the crown is 14.3 mm and the height of the crown is 15.1 mm. KPG-M 60 is missing the protocone due to breakage and there is no trace of a metacone, but there is a distinct anterior fovea at the base of the crown and there is a narrow buccal cingulum. There is an oblique wear facet exposing dentine on the anterior surface of the crown. The orientation of this facet, made by the trigonid of the opposing  $M_3$ , and the direction of wear across the facet show that the  $M^3$  crown was oriented obliquely relative to preceding molars as is typical of primitive protocetids like *Artiocetus clavis* (GSP-UM 3458; Gingerich et al., 2001a).

KPO-M 112 (Fig. 13.4, 13.5) is the centrum of an anterior thoracic vertebra. The centrum measures 34.2 mm in length, 34.4 mm in breadth, and 31.8 mm in height. KPG-M 103 (Fig. 13.6, 13.7) is the centrum of a posterior vertebra. Here the centrum measures 37.9 mm in length, 42.3 mm in width, and 27.9 mm in height. Both vertebral centra have anterior and posterior facets for rib capitula, and a broad and flat dorsal surface between widely spaced pedicles for the neural arch. KPO-M 112 is more heart-shaped in cross section, which is why it is identified as an anterior

thoracic. KPG-M 103 is more reniform in cross section, which is why it is identified as a posterior thoracic.

**Remarks.**—KPG-M 60 is seemingly too small to represent an  $M^3$  of *Togocetus traversei* and it is more likely to be an upper molar of the taxon represented by the smaller thoracic vertebrae, KPO-M 112 and KPG-M 103, described here. All three specimens are the right size to represent an indeterminate protocetid species at Kpogamé smaller than *Togocetus traversei*.

#### Protocetid indeterminate (large)

**Referred specimen.**—Tooth KPG-M 2 from Kpogamé, Togo.

**Description.**—KPG-M 2 (Fig. 13.8–13.10) is a complete right upper canine ( $C^1$ ), with a crown that measures 32.2 mm in length, 15.2 mm in width, and 33.2 mm in height. The crown and root are both elongated anteroposteriorly in a way that is distinctive of protocetid specimens interpreted as male.

**Remarks.**—KPG-M 2 is too large to belong to *Togocetus traversei*, and it appears to indicate the presence of a third protocetid species at Kpogamé.

#### Order SIRENIA Illiger, 1811

##### Family PROTOSIRENIDAE

#### Protosirenid indeterminate

**Referred specimen.**—A single protosirenid specimen, KPG-M 108, is known from Kpogamé in Togo.

**Description.**—KPG-M 108 (Fig. 14.1–14.3) is a vertebral centrum similar in size to those of *Togocetus traversei*. The centrum measures 58.4 mm in length, 59.3 in width, and 43.7 mm in height. It has several distinctive features on the dorsal surface, including neural arch pedicles set widely apart, a midline torus, and anteroposteriorly oriented sulci filling the space between the midline torus and the more laterally positioned pedicles. The centrum preserves the bases of transverse processes more robust than those of any lumbar or caudal, and KPG-M 108 must be a sacral centrum. Finally, the posterior articular surface is pentagonal to hexagonal in outline, with most angles being well defined but the ventral surface being more smoothly curved than angular. Cortical bone is seemingly thin everywhere (generally only about 1 mm thick), with cancellous bone showing wherever the surface is broken.

**Remarks.**—KPG-M 108 is very similar in size and shape to sacral centra of *Protosiren smithae* known from Egypt (Domning and Gingerich, 1994; Zalmout and Gingerich, 2012).

The combination of pedicles set widely apart, a midline torus flanked by lateral sulci, a pentagonal to hexagonal posterior

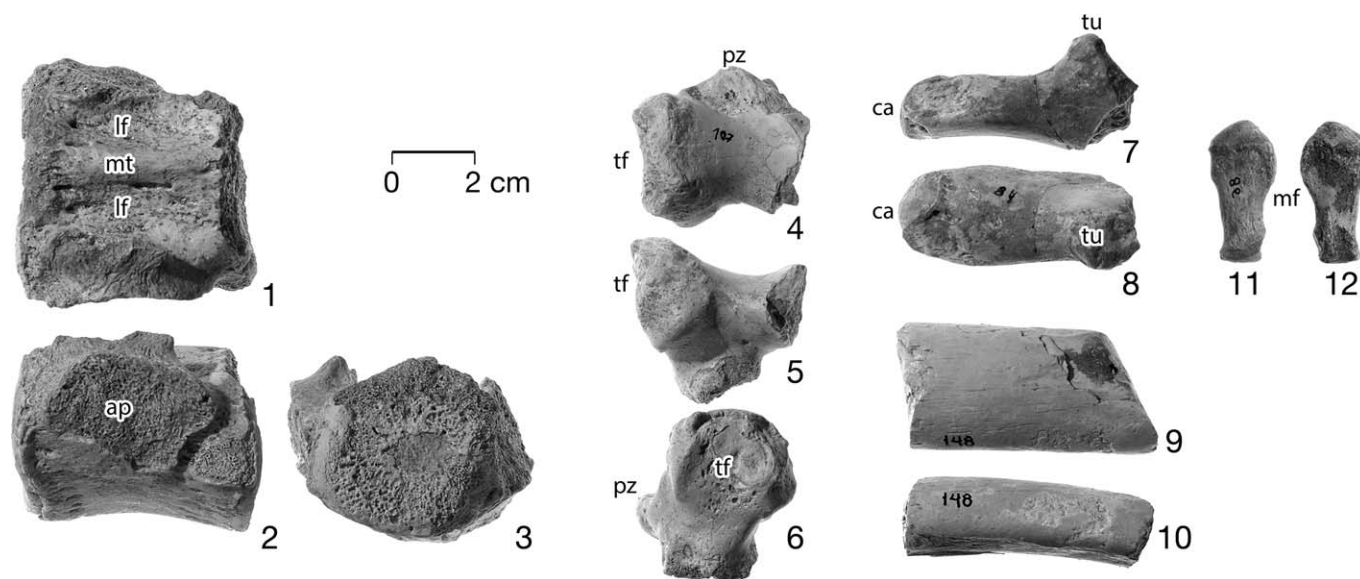


FIGURE 14—Hind limb elements of middle Lutetian protosirenid (1–3) and dugongid (4–12) sirenians from Kpogamé-Hahotoé. 1–3, KPG-M 108, centrum of a sacral vertebra, S1, in dorsal, left lateral, and posterior views (note dorsal midline torus flanked by broad lateral fossae); 4–6, KPG-M 107, left neural arch of a thoracic vertebra in dorsal, posterior, and left lateral views; 7, 8, KPG-M 84, head, neck, and tubercle of a right rib in posterior and dorsal views; 9, 10, KPO-M 148, midshaft portion of an osteosclerotic rib in lateral and anterior or posterior views; 11, 12, KPG-M 98, right metacarpal I in dorsal and plantar views. Abbreviations: *ap*=base of auricular process (transverse process); *ca*=caput or head; *lf*=lateral fossa; *mf*=medial flange; *mt*=midline torus; *pz*=prezygapophysis; *tf*=tubercular facet; *tu*=tubercle.

articular surface, and thin cortical bone is characteristic of protosirenids.

#### Family DUGONGIDAE Gray, 1821 Dugongid indeterminate

**Referred specimens.**—Eight specimens of a dugongid are known from Kpogamé in Togo: KPG-M 84, KPG-M 91, KPG-M 98, KPG-M 107, KPO-M 148, KPO-M 149, KPG-M 159, and KPG-M 160.

**Description.**—KPG-M 107 (Fig. 14.4–14.6) is much of the left half of the massive neural arch of an anterior thoracic vertebra. The size of the neural canal cannot be measured, but the lamina lateral to this is 23.0 mm in length anteroposteriorly and 21.1 mm in width mediolaterally, and the neural arch dorsolateral to the neural canal measures 29.9 mm in length anteroposteriorly and 18.9 mm in thickness dorsoventrally. The prezygapophysis on the anterior surface of the neural arch is small, about 11.0 mm in diameter, and faces dorsally. The tubercular surface for rib articulation on the lateral portion of the neural arch is much larger, about 21.0 mm in diameter, and faces laterally. The width of the vertebra across these tubercular surfaces was minimally  $2 \times 42.3 = 84.6$  mm, and the width may have been greater than this. Within the tubercular surface, there is a smaller  $15.5 \times 11.4$  mm smooth facet for the synovial capsule that matched a similarly smooth facet on the rib tubercle. The entire metapophysis or tubercular process supporting the tubercular surface is 33.8 mm in diameter anteroposteriorly, and rises some 15 mm from the neural arch proper. Bone exposed where the neural arch is broken is osteosclerotic with no cancellous bone evident.

KPG-M 84 and KPG-M 91 are both the head, neck, and tubercle of a right rib. KPG-M 84 (Fig. 14.7, 14.8) is the better preserved. The head of rib KPG-M 84 has a convex articular surface measuring 15.3 by 13.8 mm on the anteromedial side for articulation with the preceding vertebra, and a flat capitular facet measuring 18.4 by 12.5 mm on the posteromedial side for articulation with the corresponding vertebra. The neck between the capitular facet and corresponding tubercular facet is 32.0 mm

long. The tubercular facet measures only 12.5 by 8.3 mm, and there is a shallow depression dorsal to the tubercular facet for ligamentous connection to the dorsal surface of the vertebral metapophysis. The rib cross section, where broken medial to the tubercle, is mostly osteosclerotic but there is cancellous bone in a narrow crescent of the anterior cross section.

KPO-M 148, KPO-M 149, KPG-M 159, and KPG-M 160 are all blocky portions of osteosclerotic ribs. The one illustrated here, KPO-M 148 (Fig. 14.9, 14.10), 57.8 mm long, is the thickest in cross section at 29.5 mm wide and 19.5 mm thick. Comparable cross-section measurements for KPO-M 149, KPG-M 159, and KPG-M 160 are 28.1 by 15.8, 29.5 by 11.0, and 32.9 by 12.9, respectively.

KPG-M 98 (Fig. 14.11, 14.12) is a right first metacarpal, Mc-I, of a dugongid. This is 33.5 mm long, 15.9 mm wide and 8.2 mm thick at the base, and 10.0 mm wide and 7.0 mm thick at the distal end. The minimum width is 10.0 mm and minimum thickness is 5.3 mm measured between the two ends. The proximal articular surface is convex and wraps around the proximal end of the bone on the dorsal and plantar surfaces. In addition, the proximal articular surface is oblique, with the articular surface making an angle of about  $45^\circ$  with the long axis of the shaft. The distal articular surface, in contrast, wraps around the distal end of the bone on the plantar surface only, and this articular surface is perpendicular to the long axis of the shaft. There is a large proximomedial flange of bone for abduction of Mc-I away from the rest of the hand.

**Remarks.**—All of the skeletal elements described here are typical of middle and late Eocene dugongids like *Eotheroides* and *Eosiren* (Zalmout and Gingerich, 2012). Interestingly, there are no pachyostotic ribs preserved like the banana-shaped anterior ribs of *Eotheroides*. Ribs preserved here are more similar to those of *Eosiren*, but specimens at hand are insufficient to constrain identification to genus. Full osteosclerosis of the rib shaft is a distinctive feature of sirenians not found in Eocene archaeocetes.

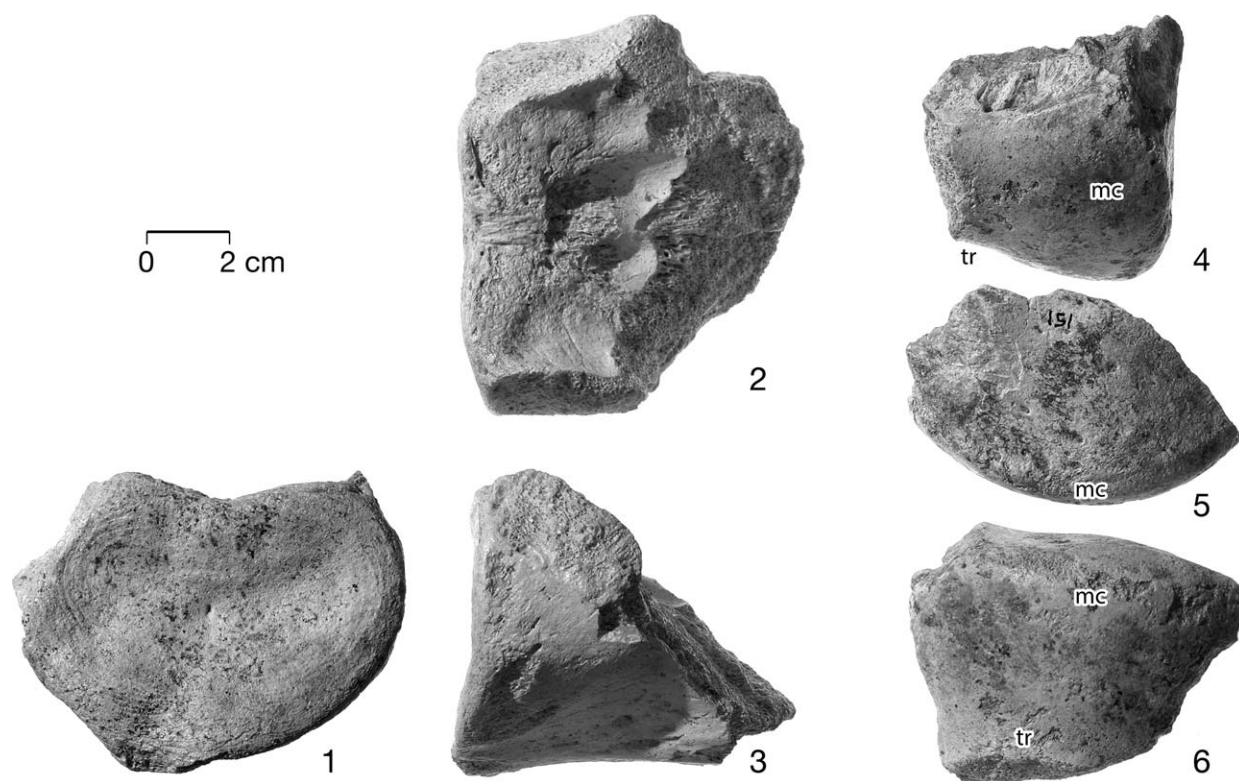


FIGURE 15—Postcranial elements of a large *Barytherium*-sized land mammal. 1–3, KPO-M 121, anterior portion of a lumbar vertebral centrum in anterior, dorsal, and lateral views; 4–6, KPO-M 151, medial condyle and portion of the trochlea of a right distal humerus in anterior, medial, and distal views. Abbreviations: *mc*=medial condyle; *tr*=trochlea.

#### Order indeterminate

*Referred specimens.*—KPO-M 121 and KPO-M 151 are two bones from Kpogamé in Togo representing an animal or animals larger than any others described here.

*Description.*—KPO-M 121 (Fig. 15.1–15.3) is the anterior portion of an incomplete vertebral centrum. The base of a slender transverse process is preserved on the right side, indicating that the vertebra is almost certainly a lumbar. The length of the centrum cannot be measured. The anterior articular surface is 96.1 mm wide and 73.1 mm high. Pedicles of the neural arch are widely spaced. The dorsal surface of the centrum has no midline torus, but an anteroposteriorly elongated depression flanks the midline on each side. These do not bear nutrient foramina. The ventral surface of the bone has a hypapophysis-like raised area on the midline that widens posteriorly. Cortical bone ranges from 1 to 3 mm thick, and the body itself is cancellous.

KPO-M 151 (Fig. 15.4–15.6) is the medial condyle and portion of the trochlea of a right distal humerus. The medial condyle is about 56 mm wide and has a radius of curvature in the parasagittal plane of about 53 mm. Cortical bone ranges from 1 to 3 mm thick, and the body itself is cancellous.

*Remarks.*—KPO-M 121 and KPO-M 151 indicate that there is a mammal in the Kpogamé fauna much larger than the cetaceans and sirenians described here. Both bones are the size expected for *Barytherium* or another large proboscidean, but these could also represent an arsinotherium or other large mammal. The distal humerus is unlike that known for any marine mammal, and the animal or animals represented were almost certainly terrestrial.

#### DISCUSSION

*Togocetus traversei* is the most interesting taxon described here. Most of its dental, cranial, and postcranial characteristics are consistent with those of a generalized protocetid. The teeth

are approximately the size of homologous teeth in *Artiocetus clavis* (GSP-UM 3458) and *Maiacetus inuus* (GSP-UM 3475 and 3551), indicating a protocetid similar in size, with a body weight estimated to have been 300–400 kg in life (Gingerich et al., 2001a, 2009).

The cranium of *Togocetus* had a well developed frontal shield, a derived characteristic of protocetids. The frontal shield of *Togocetus* measures approximately 180 mm in width across the supraorbital processes. For comparison, the type skulls of similar-sized *Artiocetus clavis* (GSP-UM 3458), *Maiacetus inuus* (GSP-UM 3475), and *Protocetus atavus* (SMNS 11084; Fraas, 1904) have frontal shields 157 mm, 165 mm, and 167 mm wide, respectively. The more advanced protocetid *Rodhocetus kasranii* (GSP-3012), which is only slightly larger, had a frontal shield 195 mm wide (Gingerich et al., 1994), and *Qaisracetus arifi* had a frontal shield 210 mm wide (GSP-UM 3410; Gingerich et al., 2001b).

The most surprising, and therefore most interesting, characteristic of *Togocetus traversei* is the small mandibular canal seen in the holotype, KPG-M 1 (Fig. 6.4, 6.5). Pakicetidae have the smallest mandibular canals, Protocetidae have canals of intermediate size, and Basilosauridae have the largest canals relative to tooth size among archaeocetes (Fig. 16). Mandibular canal enlargement is normally thought to be integral to evolution of an auditory system capable of hearing efficiently in water (Norris, 1968). The other component of the auditory system documented here, the tympanic bulla, is at the functional stage expected for a protocetid. Combination of a small mandibular canal with a large, dense, osteosclerotic bulla, a combination unique to *Togocetus traversei*, shows that these two anatomical features are not as tightly linked in terms of function to hearing as previously thought.



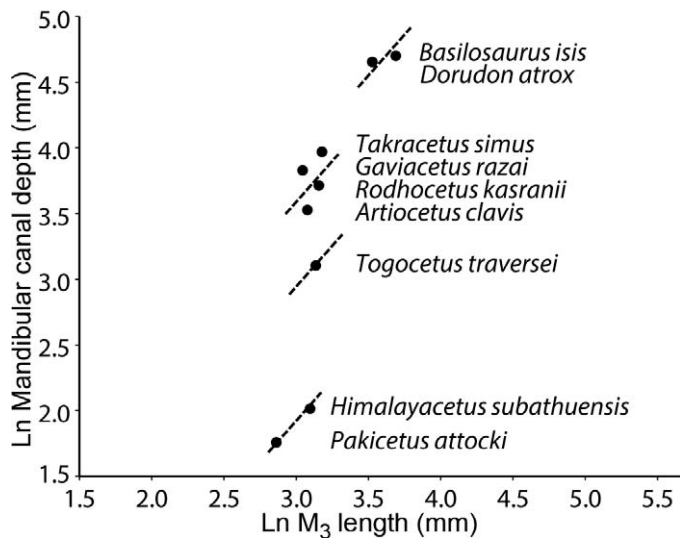


FIGURE 16—Comparison of mandibular canal depth at the position of  $M_3$  in *Togocetus traversei* with that in early-to-middle Eocene pakicetid archaeocetes (*Pakicetus* and *Himalayacetus*), typical middle Eocene protocetids (*Artiocetus*, *Rodhocetus*, *Gaviacetus*, and *Takaracetus*), and late Eocene basilosaurids (*Dorudon* and *Basilosaurus*). Dashed lines represent isometry within each group. Note that there is a progressive trend toward increasing mandibular canal depth through time even when controlling for increasing tooth size (and by implication increasing body size). *Togocetus* is distinctly primitive for a protocetid in having a small mandibular canal, even though its age and adaptive grade are similar to those of other early protocetids.

Another distinctive feature of *Togocetus traversei* is seen in the dentition, where the first lower molar,  $M_1$ , retains a salient metaconid cusp posterior to the protoconid (Figs. 4.7, 5.13). The functional significance of the metaconid is not clear.

The postcranial skeleton of *Togocetus traversei* exhibits the relatively long cervical centra, mobile shoulder, digitigrade manus, large pelvis, well-developed hind limbs, and feet specialized for swimming that are typical for Protocetidae. The spherical head of the humerus, the large greater and lesser tubercles, and the deep bicipital groove separating these (Fig. 10.5–10.9) indicate a heavily muscled shoulder. Similarly, the broad distal femur, broad patellar groove and posteriorly positioned femoral condyles on the femur, and the deep groove for the flexor digitorum longus tendon on the tibia indicate a heavily muscled knee (Fig. 11.1–11.10).

*Togocetus traversei* lacks a fovea for the teres ligament on the femoral head. This fovea is typically present in land mammals (Jenkins and Camazine, 1977), it is present in pakicetid archaeocetes (Madar, 2007), and it is present in all other protocetids for which the femur is known. Absence of a fovea capitis femoris indicates loss of the teres ligament, which normally maintains the femoral head within the acetabulum of the pelvis in mammals that have weight-bearing hip joints (Adam, 2009). This observation, combined with indications of heavily muscled shoulder and knee joints, suggests that *Togocetus traversei* was unusual in being a more aquatic foot-powered swimmer than most protocetids.

The phosphate deposits at Kpogamé-Hahotoé are richly fossiliferous, and much of the bone found there is exceptionally well preserved. We expect further work at the site might enable recovery of more complete specimens before they are damaged by mining equipment, which would undoubtedly repay the effort required. Bourdon and Cappetta (2012) recently described an odontopterygiform bird from Kpogamé. Hautier et al. (2012)

identified a possible middle Eocene prorastomid sirenian from phosphate deposits in Senegal, and hence Kpogamé-Hahotoé may also yield prorastomids in the future. It is likely to yield additional surprises in terms of Eocene vertebrate remains.

In conclusion, *Togocetus traversei* was similar to other protocetid archaeocetes in many dental and osteological characteristics, but it also exhibits an otherwise unknown mosaic of retained primitive characteristics (small mandibular canal, metaconid on  $M_1$ ) and derived specializations indicating adaptation to life in water (loss of the fovea capitis femoris and loss of the teres ligament stabilizing the hip). Here we have separated specimens that clearly represent a minimum of three protocetid archaeocetes, a protosirenid sirenian, a dugongid sirenian, and a large land mammal. The diversity of marine mammals present at Kpogamé indicates that by Lutetian early middle Eocene time protocetid archaeocetes had dispersed far from their postulated early Eocene origin in the eastern Tethys Sea of Indo-Pakistan (Gingerich et al., 1983; Bajpai and Gingerich, 1998), and both protosirenid and dugongid sirenians had dispersed far from their postulated early Eocene origin in the Caribbean Sea (Domning, 2001). Both orders, Cetacea and Sirenia, were marine and became widely distributed geographically during early middle Eocene time.

#### ACKNOWLEDGMENTS

Many of the specimens described here were collected by our late colleague Michel Traverse of Bourg de Lignerolles in France. We anticipated co-authoring this contribution with him, but consider it a more fitting honor to name the best of the archaeocetes known from Kpogamé-Hahotoé for him. We thank Mr. N. Péré, Directeur Général de Mines et de la Géologie du Togo, and Mr. O. Bagnah, Directeur de l'Office Togolais des Phosphates, for facilities provided in the field and in the mining city of Hahotoé. Field work in Togo was supported by the 'Géologie et Géophysique des Océans' program of CNRS (PIROCEAN). We thank Dr. E. Heizmann for access to *Protocetus atavus* and other archaeocete specimens at the Staatliches Museum für Naturkunde in Stuttgart. Dr. E. Fordyce, an anonymous referee, and journal editors provided critical reviews improving the manuscript. Togo specimens were prepared by William J. Sanders, and final illustrations were prepared by Bonnie Miljour, both at the University of Michigan. This research was supported by several grants from the National Geographic Society, most recently, 7226-04, and from the U. S. National Science Foundation, most recently EAR-0920972.

#### REFERENCES

- ABEL, O. 1907. The genealogical history of the marine mammals. Annual Report of the Smithsonian Institution, 1907:473–496.
- ADAM, P. J. 2009. Hind limb anatomy, p. 562–565. In W. F. Perrin, B. Würsig, and J. G. M. Thewissen (eds.), *Encyclopedia of Marine Mammals*, Second Edition. Academic-Elsevier Press, San Diego.
- ADNET, S., H. CAPPETTA, AND R. TABUCE. 2010. A middle-late Eocene vertebrate fauna (marine fish and mammals) from southwestern Morocco; preliminary report: age and palaeobiogeographical implications. *Geological Magazine*, 147:860–870.
- ANDREWS, C. W. 1920. A description of new species of zeuglodont and of leathery turtle from the Eocene of southern Nigeria. *Proceedings of the Zoological Society of London*, 1919:309–319.
- ASTIBIA, H., N. BARDET, X. PEREDA-SUBERBIOLA, A. PAYROS, V. D. BUFFRÉNIL, J. ELORZA, J. TOSQUELLA, A. BERRETEAGA, AND A. BADIOLA. 2010. New fossils of Sirenia from the middle Eocene of Navarre (western Pyrenees): the oldest west European sea cow record. *Geological Magazine*, 147:665–673.
- BAJPAI, S., D. P. DOMNING, D. P. DAS, AND V. P. MISHRA. 2009. A new middle Eocene sirenian (Mammalia, Protosirenidae) from India. *Neues Jahrbuch für Geologie und Paläontologie, Abhandlungen*, 252/3:257–267.
- BAJPAI, S. AND P. D. GINGERICH. 1998. A new Eocene archaeocete (Mammalia, Cetacea) from India and the time of origin of whales. *Proceedings of the National Academy of Sciences U.S.A.*, 95:15464–15468.

- BAJPAI, S., J. G. M. THEWISSEN, V. V. KAPUR, B. N. TIWARI, AND A. SAHNI. 2006. Eocene and Oligocene sirenians (Mammalia) from Kachchh, India. *Journal of Vertebrate Paleontology*, 26:400–410.
- BERGGREN, W. A. AND P. N. PEARSON. 2005. A revised tropical to subtropical Paleogene planktonic foraminiferal zonation. *Journal of Foraminiferal Research*, 35:279–298.
- BOURDON, E. AND H. CAPPETTA. 2012. Pseudo-toothed birds (Aves, Odontopterygiformes) from the Eocene phosphate deposits of Togo, Africa. *Journal of Vertebrate Paleontology*, 32:965–970.
- BRISSON, M.-J. 1762. *Regnum Animale in Classes IX. Distributum, sive Synopsis Methodica*. Lugduni Batavorum, Theodorum Haak, Leiden, 296 p.
- CAPPETTA, H. AND M. TRAVERSE. 1988. Une riche faune de sélachiens dans le bassin à phosphate de Kpogamé-Hahotoé (Éocène moyen du Togo): note préliminaire et précisions sur la structure et l'âge du gisement. *Geobios*, Lyon, 21:359–365.
- DOMNING, D. P. 2001. The earliest known fully quadrupedal sirenian. *Nature*, 413:625–627.
- DOMNING, D. P. AND P. D. GINGERICH. 1994. *Protosiren smithae*, new species (Mammalia, Sirenia), from the late middle Eocene of Wadi Hitán, Egypt. Contributions from the Museum of Paleontology, University of Michigan, 29:69–87.
- DOMNING, D. P., G. S. MORGAN, AND C. E. RAY. 1982. North American Eocene sea cows (Mammalia: Sirenia). *Smithsonian Contributions to Paleobiology*, 52:1–69.
- ELOUARD, P. 1981. Découverte d'un archéocète dans les environs de Kaolack. *Notes Africaines*, Dakar, 109:8–10.
- FRAAS, E. 1904. Neue Zeuglodonten aus dem unteren Mitteleocän vom Mokattam bei Cairo. *Geologische und Paläontologische Abhandlungen*, Jena, 6:197–220.
- GINGERICH, P. D. 2010. Cetacea, p. 873–899. In L. Werdelin and W. J. Sanders (eds.), *Cenozoic Mammals of Africa*. University of California Press, Berkeley.
- GINGERICH, P. D., H. CAPPETTA, AND M. TRAVERSE. 1992. Marine mammals (Cetacea and Sirenia) from the middle Eocene of Kpogamé-Hahotoé in Togo (abstract). *Journal of Vertebrate Paleontology*, 12A:29–30.
- GINGERICH, P. D., M. HAQ, I. H. KHAN, AND I. S. ZALMOUT. 2001b. Eocene stratigraphy and archaeocete whales (Mammalia, Cetacea) of Drug Lahar in the eastern Sulaiman Range, Balochistan (Pakistan). Contributions from the Museum of Paleontology, University of Michigan, 30:269–319.
- GINGERICH, P. D., M. HAQ, W. V. KOENIGSWALD, W. J. SANDERS, B. H. SMITH, AND I. S. ZALMOUT. 2009. New protocetid whale from the middle Eocene of Pakistan: birth on land, precocial development, and sexual dimorphism. *PLoS ONE*, 4 (e4366):1–20.
- GINGERICH, P. D., M. HAQ, I. S. ZALMOUT, I. H. KHAN, AND M. S. MALKANI. 2001a. Origin of whales from early artiodactyls: hands and feet of Eocene Protocetidae from Pakistan. *Science*, 293:2239–2242.
- GINGERICH, P. D., S. M. RAZA, M. ARIF, M. ANWAR, AND X. ZHOU. 1994. New whale from the Eocene of Pakistan and the origin of cetacean swimming. *Nature*, 368:844–847.
- GINGERICH, P. D., N. A. WELLS, D. E. RUSSELL, AND S. M. I. SHAH. 1983. Origin of whales in epicontinental remnant seas: new evidence from the early Eocene of Pakistan. *Science*, 220:403–406.
- GRAY, J. E. 1821. On the natural arrangement of vertebrate animals. *London Medical Repository Monthly Journal and Review*, 15:296–310.
- HALSTEAD, L. B. AND J. A. MIDDLETON. 1974. New material of the archaeocete whale, *Pappocetus lugardi* Andrews, from the middle Eocene of Nigeria. *Journal of Mining and Geology*, 8:81–85.
- HALSTEAD, L. B. AND J. A. MIDDLETON. 1976. Fossil vertebrates of Nigeria. Part II, 3.4. Archaeocete whale: *Pappocetus lugardi* Andrews, 1920. *Nigerian Field*, 41:131–133.
- HAUTIER, L., R. SARR, R. TABUCE, F. LIHOREAU, S. ADNET, D. P. DOMNING, M. SAMB, AND P. M. HAMEH. 2012. First prorastomid sirenian from Senegal (western Africa) and the Old World origin of sea cows. *Journal of Vertebrate Paleontology*, 32:1218–1222.
- ILLIGER, C. 1811. *Prodromus systematis mammalium et avium additis terminis zoographicis utriusque classis*. C. Salfeld, Berlin, 301 p.
- JENKINS, F. A. AND S. M. CAMAZINE. 1977. Hip structure and locomotion in ambulatory and cursorial carnivores. *Journal of Zoology*, London, 181:351–370.
- JOHNSON, A. K., P. RAT, AND J. LANG. 2000. Le bassin sédimentaire à phosphates du Togo (Maastrichtien-Eocène): stratigraphie, environnements et évolution. *Journal of African Earth Sciences*, 30:183–200.
- KILINC, M. AND P. COTILLON. 1977. Le gisement d'Hahotoé-Kpogamé (Tertiaire du Sud Togo) exemple de piège sédimentaire à sables phosphatés. *Bulletin du Bureau de Recherches Géologiques et Minières*, Deuxième Série, 1:43–63.
- KUMAR, K. AND A. SAHNI. 1986. *Remingtonocetus harudiensis*, new combination, a middle Eocene archaeocete (Mammalia, Cetacea) from western Kutch, India. *Journal of Vertebrate Paleontology*, 6:326–349.
- MADAR, S. I. 2007. The postcranial skeleton of early Eocene pakicetid cetaceans. *Journal of Paleontology*, 81:176–200.
- MADAR, S. I., J. G. M. THEWISSEN, AND S. T. HUSSAIN. 2002. Additional holotype remains of *Ambulocetus natans* (Cetacea, Ambulocetidae), and their implications for locomotion in early whales. *Journal of Vertebrate Paleontology*, 22:405–422.
- MCLEOD, S. A. AND L. G. BARNES. 2008. A new genus and species of Eocene protocetid archaeocete whale (Mammalia, Cetacea) from the Atlantic Coastal Plain. *Natural History Museum of Los Angeles County Science Series*, 41:73–98.
- MEAD, J. G. AND R. E. FORDYCE. 2009. The therian skull: a lexicon with emphasis on the odontocetes. *Smithsonian Contributions to Zoology*, 627: 1–248.
- NORRIS, K. S. 1968. The evolution of acoustic mechanisms in odontocete cetaceans, p. 297–324. In E. T. Drake (ed.), *Evolution and Environment*. Yale University Press, New Haven.
- NUMMELA, S., S. T. HUSSAIN, AND J. G. M. THEWISSEN. 2006. Cranial anatomy of Pakicetidae (Cetacea, Mammalia). *Journal of Vertebrate Paleontology*, 26: 746–759.
- OWEN, R. 1855. On the fossil skull of a mammal (*Prorastomus sirenioides* Owen) from the island of Jamaica. *Quarterly Journal of the Geological Society of London*, 11:541–543.
- OWEN, R. 1875. On fossil evidences of a sirenian mammal (*Eotherium aegyptiacum*) from the nummulitic Eocene of the Mokattam cliffs, near Cairo. *Quarterly Journal of the Geological Society of London*, 31:100–105.
- SAHNI, A. AND V. P. MISHRA. 1975. Lower Tertiary vertebrates from western India. *Palaeontological Society of India, Monographs*, 3:1–48.
- SLANSKY, M. 1962. Contribution à l'étude géologique du bassin sédimentaire côtier du Dahomey et du Togo. *Mémoires du Bureau de Recherches Géologiques et Minières*, Orléans, 11:1–270.
- SLANSKY, M. 1980. Géologie des phosphates sédimentaires. *Mémoires du Bureau de Recherches Géologiques et Minières*, Orléans, 114:1–92.
- STROMER, E. 1908. Die Archaeoceti des ägyptischen Eozäns. Beiträge zur Paläontologie und Geologie Österreich-Ungarns und des Orients, Vienna, 21:106–178.
- STROMER, E. 1910. Reptilien- und Fischreste aus dem marinen Alttertiär von Südtogo (Westafrika). *Zeitschrift der Deutschen Geologischen Gesellschaft, Monatsberichte*, Stuttgart, 62:478–507.
- THEWISSEN, J. G. M., S. T. HUSSAIN, AND M. ARIF. 1994. Fossil evidence for the origin of aquatic locomotion in archaeocete whales. *Science*, 263:210–212.
- THEWISSEN, J. G. M., S. I. MADAR, AND S. T. HUSSAIN. 1996. *Ambulocetus natans*, an Eocene cetacean (Mammalia) from Pakistan. *Courier Forschungsinstitut Senckenberg, Frankfurt am Main*, 191:1–86.
- VANDENBERGE, N., F. J. HILGEN, AND R. P. SPEIJER. 2012. The Paleogene period, p. 855–921. In F. M. Gradstein, J. G. Ogg, M. D. Schmitz, and G. M. Ogg (eds.), *The Geological Time Scale 2012*. Elsevier, Amsterdam.
- WILLIAMS, E. M. 1998. Synopsis of the earliest cetaceans: Pakicetidae, Ambulocetidae, Remingtonocetidae, and Protocetidae, p. 1–28. In J. G. M. Thewissen (ed.), *The Emergence of Whales: Evolutionary Patterns in the Origin of Cetacea*. Plenum, New York.
- ZALMOUT, I. S. AND P. D. GINGERICH. 2012. Late Eocene sea cows (Mammalia, Sirenia) from Wadi Al Hitán in the Western Desert, Fayum, Egypt. *University of Michigan Papers on Paleontology*, 37:1–158.
- ZALMOUT, I. S., M. HAQ, AND P. D. GINGERICH. 2003. New species of *Protosiren* (Mammalia, Sirenia) from the early middle Eocene of Balochistan (Pakistan). Contributions from the Museum of Paleontology, University of Michigan, 31:79–87.

ACCEPTED 27 JUNE 2013